		L	T	P	C
18PHP105A	**MATERIALS CHARACTERIZATION**	**4**	**-**	**-**	**4**

SCOPE: Study of materials is always important, for any application, including fabrication of satellites. It is important to know the basics of materials and their formation, for a physics student.

OBJECTIVE: To introduce various methods available for characterizing the materials. The characterization of materials specifically addresses that portfolio with which researchers and educators must have working familiarity.

UNIT I

X-Ray Techniques

Introduction, X-Ray Powder Diffraction - Particle size - strain determination, Single Crystal X-Ray Structure Determination, GIXRD and its applications, X-Ray Photoelectron Spectroscopy, Surface X-Ray Diffraction.

Neutron Techniques

Introduction, Neutron Powder Diffraction, Single Crystal Neutron Diffraction.

UNIT II

Thermal Analysis

Introduction - Definitions, Codes of Practice and Nomenclature - thermogravimetric analysis (TGA) - instrumentation - determination of weight loss and decomposition products - differential thermal analysis (DTA) - cooling curves - differential scanning calorimetry (DSC) - instrumentation - specific heat capacity measurements - determination of thermomechanical parameters .

UNIT III

Magnetic Analysis

Vibrating sample magnetometer - SQUID : Introduction - construction and working principle.

Optical Microscopy

Optical microscopy techniques - Bright field - Dark field optical microscopy - phase contrast microscopy -differential interference contrast microscopy - fluorescence microscopy - confocal microscopy - Metallurgical microscope.

UNIT IV

Electron Microscopy

Electron diffraction technique – High energy electron diffraction – Low energy electron diffraction - Electron microscopy – Scanning electron microscopy (SEM) - FESEM - EDAX - TEM - HRTEM: working principle and Instrumentation - sample preparation - Advantages/disadvantages.

Scanning Probe Microscopy

Scanning probe microscopy - STM - AFM - EPMA - working principle and Instrumentation - Advantages/disadvantages.

UNIT V

Electrical and Optical Methods of Characterisation

Two probe and four probe methods - van der Pauw method - Hall probe and measurement - scattering mechanism - C-V, I-V characteristics - Schottky barrier capacitance - impurity concentration - electrochemical C-V profiling - limitations - Introduction to Photoluminescence and Electroluminescence - Applications. Dielectrics - working principle and Instrumentation - Applications.

Suggested Reading Books

1. Elton N. Kaufmann, Characterization of Materials volumes 1 and 2, John Wiley & Sons, Inc., Hoboken, New Jersey, 2003.
2. R.A.Stradling and P.C.Klipstain. Growth and Characterization of semiconductors. Adam Hilger, Bristol, 1990.
3. Cullity B D., Stock S R “Elements of X-ray Diffraction”, Prentice Hall, Inc 2001.
4. J.A.Belk. Electron Microscopy and Microanalysis of Crystalline Materials. Applied Science Publishers, London, 1979.
5. L. E.Murr. Electron and Ion microscopy and Microanalysis principles and Applications. Marcel Dekker Inc., New York, 1991.
6. D.Kealey & P.J.Haines, Analytical Chemistry, Viva Books Private Limited, New Delhi, 2002. 5. Banwell, Fundamentals of Molecular Spectroscopy, McGraw-Hill Education, Pvt. Ltd., 2013.

KARPAGAM ACADEMY OF HIGHER EDUCATION
(Deemed to be University Established Under Section 3 of UGC Act 1956)
Coimbatore – 641 021.

LECTURE PLAN
DEPARTMENT OF PHYSICS

STAFF NAME : **Dr. S. KARUPPUSAMY**
SUBJECT NAME: **MATERIALS CHARACTERIZATION** SUB.CODE: **18PHP105A**
SEMESTER: **I** CLASS: **I M.Sc., (PHYSICS)**

Sl.No.	**Lecture Duration Period**	**Topics to be covered**	**Support Material/Page Nos.**
UNIT I			
1.	1 hr	**X-Ray Techniques** Introduction, X-Ray Powder Diffraction	T1(835)
2.	1 hr	Particle size - strain determination,	J1
3.	1 hr	Single Crystal X-Ray Structure Determination,	T1(850)
4.	1 hr	GIXRD and its applications	
5.	1 hr	X-Ray Photoelectron Spectroscopy	T1(970)
6.	1 hr	Surface X-Ray Diffraction	T1(1007
7.	1 hr	**Neutron Techniques** Introduction, Neutron Powder Diffraction	T1(1285)
8.	1 hr	Single Crystal Neutron Diffraction.	T1(1307)
9.	1 hr	Revision	
Total Number of Hours Planned For Unit I = 9			
UNIT II			
10.	1 hr	**Thermal Analysis** Introduction - Definitions, Codes of Practice and Nomenclature	T1 (337-344)
11.	1 hr	thermogravimetric analysis (TGA) - instrumentation	T1(344-360)

12.	1 hr	determination of weight loss and decomposition products	T1(352-360)
13.	1 hr	differential thermal analysis (DTA) - cooling curves	T1(362-370)
14.	1 hr	differential scanning calorimetry (DSC) – instrumentation	T1(362-370)
15.	1 hr	specific heat capacity measurements	T1(362-370)
16.	1 hr	determination of thermomechanical parameters	T1(362-370)
17.	1 hr	Revision	
Total Number of Hours Planned For Unit II = 8			
UNIT III			
18.	1 hr	**Magnetic Analysis** Vibrating sample magnetometer	W1
19.	1 hr	SQUID : Introduction - construction and working principle	W2
20.	1 hr	**Optical Microscopy** Optical microscopy techniques	T1(665-667)
21.	1 hr	Bright field - Dark field optical microscopy - phase contrast microscopy	T1(665-667)
22.	1 hr	differential interference contrast microscopy	T1(665-667)
23.	1 hr	fluorescence microscopy - confocal microscopy	T1(665-667)
24.	1 hr	Metallurgical microscope	T1(665-667)
25.	1 hr	Revision	
Total Number of Hours Planned For Unit III = 8			
UNIT IV			
26.	1 hr	**Electron Microscopy** Electron diffraction technique - working principle and Instrumentation	T1(1049)
27.	1 hr	High energy electron diffraction – Low energy electron diffraction	T1(1120)
28.	1 hr	Electron microscopy – Scanning electron microscopy (SEM)	T1(1050)
29.	1 hr	FESEM – EDAX	W3

30.	1 hr	TEM - HRTEM - sample preparation - Advantages/disadvantages.	T1(1063)
31.	1 hr	**Scanning Probe Microscopy** Scanning probe microscopy - working principle and Instrumentation	W4
32.	1 hr	STM	T1(1111)
33.	1 hr	AFM	W5
34.	1 hr	EPMA - Advantages/disadvantages	W6
35.	1 hr	Revision	
Total Number of Hours Planned For Unit IV = 10			
UNIT V			
36.	1 hr	**Electrical and Optical Methods of Characterization** Two probe and four probe methods	W7
37.	1 hr	Van der Pauw method	W7
38.	1 hr	Hall probe and measurement	T1(411)
39.	1 hr	scattering mechanism	T1(411)
40.	1 hr	C-V, I-V characteristics	T1(456)
41.	1 hr	Schottky barrier capacitance	T1(459)
42.	1 hr	Impurity concentration – electrochemical C-V profiling – limitations	T1(460)
43.	1 hr	Introduction to Photoluminescence and Electroluminescence – Applications	T1(427)
44.	1 hr	Dielectrics - working principle and Instrumentation – Applications	W5
45.	1 hr	Revision	
46.	1 hr	Old Question Paper Revision	
47.	1 hr	Old Question Paper Revision	
48.	1 hr	Old Question Paper Revision	
Total Number of Hours Planned For Unit V = 13			

Suggested Reading Books

1. Elton N. Kaufmann, Characterization of Materials volumes 1 and 2, John Wiley & Sons, Inc., Hoboken, New Jersey, 2003.
2. R.A.Stradling and P.C.Klipstain. Growth and Characterization of semiconductors. Adam Hilger, Bristol, 1990.
3. Cullity B D., Stock S R “Elements of X-ray Diffraction”, Prentice Hall, Inc 2001.
4. J.A.Belk. Electron Microscopy and Microanalysis of Crystalline Materials. Applied Science Publishers, London, 1979.
5. L. E.Murr. Electron and Ion microscopy and Microanalysis principles and Applications. Marcel Dekker Inc., New York, 1991.
6. D.Kealey & P.J.Haines, Analytical Chemistry, Viva Books Private Limited, New Delhi, 2002.
7. Banwell, Fundamentals of Molecular Spectroscopy, McGraw-Hill Education, Pvt. Ltd., 2013.
8. J1 - http://www.jtaphys.com/content/2251-7235/6/1/6
9. W1 - https://nptel.ac.in/courses/115103030/30
10. W2 - http://squid.iitd.ernet.in/Basic_Literature.htm
11. W3 - http://shodhganga.inflibnet.ac.in/bitstream/10603/87209/5/chapter%202.pdf
12. W4 - https://www.bruker.com/products/surface-and-dimensional-analysis/atomic-force-microscopes/campaigns/spm-microscopes-intro-to-scanning-probe-microscopy.html
13. W5 - http://shodhganga.inflibnet.ac.in/bitstream/10603/70669/11/11_chapter%204.pdf
14. W6 - https://www.cameca.com/products/epma/technique
15. W7 - https://nptel.ac.in/courses/115103030/25.

SYLLABUS

X-Ray Techniques

Introduction, X-Ray Powder Diffraction - Particle size - strain determination, Single Crystal X-Ray Structure Determination, GIXRD and its applications, X-Ray Photoelectron Spectroscopy, Surface X-Ray Diffraction.

Neutron Techniques

Introduction, Neutron Powder Diffraction, Single Crystal Neutron Diffraction.

POWDER X-RAY DIFFRACTION (PXRD)

Powder X-ray diffraction (XRD) is a rapid analytical technique primarily used for phase identification of a crystalline material and can provide information on unit cell dimensions. The analyzed material is finely ground, homogenized, and average bulk composition is determined. X-ray powder diffraction (XRD) is a rapid analytical technique primarily used for phase identification of a crystalline material and can provide information on unit cell dimensions. The analyzed material is finely ground, homogenized, and average bulk composition is determined.

Fundamental principles of Powder X-ray diffraction (PXRD)

Max von Laue, in 1912, discovered that crystalline substances act as three-dimensional diffraction gratings for X-ray wavelengths similar to the spacing of planes in a crystal lattice. X-ray diffraction is now a common technique for the study of crystal structures and atomic spacing.

X-ray diffraction is based on constructive interference of monochromatic X-rays and a crystalline sample. These X-rays are generated by a cathode ray tube, filtered to produce monochromatic radiation, collimated to concentrate, and directed toward the sample. The interaction of the incident rays with the sample produces constructive interference (and a diffracted ray) when conditions satisfy Bragg's Law ($n\lambda=2d \sin \theta$). This law relates the wavelength of electromagnetic radiation to the diffraction angle and the lattice spacing in a crystalline sample. These diffracted X-rays are then detected, processed and counted. By scanning the sample through a range of 2θ angle, all possible diffraction directions of the lattice should be attained due to the random orientation of the powdered material. Conversion of the diffraction peaks to d-spacing allows identification of the mineral because each mineral has a set of unique d-spacing. Typically, this is achieved by comparison of d-spacing with standard reference patterns.

All diffraction methods are based on generation of X-ray in an X-ray tube. These X-rays are directed at the sample, and the diffracted rays are collected. A key component of all diffraction is the angle between the incident and diffracted rays.

Instrumentation

X-ray diffractometer consist of three basic elements: an X-ray tube, a sample holder, and an X-ray detector. Bruker's X-ray Diffraction D8-Discover instrument. X-rays are generated in a cathode ray tube by heating a filament to produce electrons, accelerating the electrons toward a target by applying a voltage, and bombarding the target material with electrons. When electrons have sufficient energy to dislodge inner shell electrons of the target material, characteristic X-ray spectra are produced. These spectra consist of several components, the most common being K_α and K_β. K_α consists, in part, of $K_{\alpha1}$ and $K_{\alpha2}$. $K_{\alpha1}$ has a slightly shorter wavelength and twice the intensity as $K_{\alpha2}$. The specific wavelengths are characteristic of the target material (Cu, Fe, Mo, Cr). Filtering, by foils or crystal monochromator, is required to produce monochromatic X-rays needed for diffraction. $K_{\alpha1}$and $K_{\alpha2}$ are sufficiently close in wavelength such that a weighted average of the two is used. Copper is the most common target material for single-crystal diffraction, with CuK_α radiation = 1.5418Å. These X-rays are collimated and directed onto the sample. As the sample and detector are rotated, the intensity of the reflected X-rays is recorded. When the geometry of the incident X-rays impinging the sample satisfies the Bragg Equation, constructive interference occurs and a peak in intensity occurs. A detector records and processes this X-ray signal and converts the signal to a count rate which is then output to a device such as a printer or computer monitor. The geometry of an X-ray diffractometer is such that the sample rotates in the path of the collimated X-ray beam at an angle θ while the X-ray detector is mounted on an arm to collect the diffracted X-rays and rotates at an angle of 2θ. The instrument used to maintain the angle and rotate the sample is termed a goniometer. For typical powder patterns, data is collected at 2θ from ~5° to 70°, angles that are preset in the X-ray scan.

Applications

Powder X-ray diffraction is most widely used for the identification of unknown crystalline materials (e.g. minerals, inorganic compounds). Determination of unknown solids is critical to studies in geology, environmental science, material science, engineering and biology.

Other applications include:

i) Characterization of crystalline materials
ii) Identification of fine-grained minerals such as clays and mixed layer clays that are difficult to determine optically
iii) Determination of unit cell dimensions
iv) Measurement of sample purity

With specialized techniques, XRD can be used to:

i) Determine crystal structures using Rietveld refinement
ii) Determine of modal amounts of minerals (quantitative analysis)
iii) Characterize thin films samples by:
  a) Determining lattice mismatch between film and substrate and to inferring stress and strain
  b) Determining dislocation density and quality of the film by rocking curve measurements
  c) Measuring super lattices in multilayered epitaxial structures
  d) Determining the thickness, roughness and density of the film using glancing incidence X-ray reflectivity measurements
iv) Make textural measurements, such as the orientation of grains, in a polycrystalline sample

Strengths and Limitations of Powder X-ray diffraction (XRD)

Strengths

i) Powerful and rapid (< 20 min) technique for identification of an unknown mineral
ii) In most cases, it provides an unambiguous material determination
iii) Minimal sample preparation is required

iv) XRD units are widely available

v) Data interpretation is relatively straight forward

Limitations

i) Homogeneous and single phase material is best for identification of an unknown

ii) Must have access to a standard reference file of inorganic compounds (d-spacing, hkl)

iii) Requires tenths of a gram of material which must be ground into a powder

iv) For mixed materials, detection limit is ~ 2% of sample

v) For unit cell determinations, indexing of patterns for non-isometric crystal systems is complicated

vi) Peak overlay may occur and worsens for high angle 'reflections'.

Sample collection and preparation

Determination of an unknown requires: the material, an instrument for grinding, and a sample holder.

Obtain a few tenths of a gram (or more) of the material, as pure as possible

Grind the sample to a fine powder, typically in a fluid to minimize inducing extra strain (surface energy) that can offset peak positions, and to randomize orientation. Powder less than ~10 μm (or 200-mesh) in size is preferred

Data collection, results and presentation

Data collection

The intensity of diffracted X-rays is continuously recorded as the sample and detector rotate through their respective angles. A peak in intensity occurs when the material contains lattice planes with d-spacing appropriate to diffract X-rays at that value of θ. Although each peak consists of two separate reflections ($K\alpha_1$ and $K\alpha_2$), at small values of 2θ the peak locations overlap with $K\alpha_2$ appearing as a hump on the side of $K\alpha_1$. Greater separation occurs at higher values of θ. Typically these combined peaks are treated as one.

Data reduction

Results are commonly presented as peak positions at 2θ and X-ray counts (intensity) in the form of a table or an x-y plot (shown above). Intensity (*I*) is either reported as peak height intensity, that intensity above background, or as integrated intensity, the area under the peak. The relative intensity is recorded as the ratio of the peak intensity to that of the most intense peak.

Determination of an unknown

The d-spacing of each peak is then obtained by solution of the Bragg equation for the appropriate value of λ. Once all d-spacing have been determined, automated search/match routines compare the *d*'s of the unknown to those of known materials. Because each material has a unique set of d-spacing, matching these d-spacing provides an identification of the unknown sample. A systematic procedure is used by ordering the d-spacing in terms of their intensity beginning with the most intense peak. Files of d-spacing for hundreds of thousands of organic and inorganic compounds are available from the International Centre for Diffraction Data as the Powder Diffraction File (PDF). Commonly this information is an integral portion of the software that comes with the instrumentation.

Particle size and strain determination:

Determination of Size and Strain

The previous section explained how size and inhomogeneous strain can broaden the powder diffraction peak. A question that has occupied the minds of many powder diffractionists during the last (20th) century is whether the mean size and strain within a powder can be calculated from the diffraction pattern even when both are present simultaneously. We answer this question in both an approximate and more rigorous fashion.

Williamson-Hall Plot

This method is attributed to G.K.Williamson and his student, W.H.Hall (Acta Metall. 1, 22-31 (1953)). It relies on the principle that the approximate formulae for size broadening, β_L, and strain broadening, β_e , vary quite differently with respect to Bragg angle, θ:

$$\beta_L = \mathbf{K}\lambda$$

$$\frac{}{L\cos\theta}$$

$$\beta_e = \mathbf{C}\varepsilon\tan\theta$$

One contribution varies as 1/cosθ and the other as tanθ. If both contributions are present then their combined effect should be determined by convolution. The simplification of Williamson and Hall is to assume the convolution is either a simple sum or sum of squares (see previous discussion on Sources of Peak Broadening within this section). Using the former of these then we get:

$$\beta_{tot} = \beta_e + \beta_L = \mathbf{C}\varepsilon\tan\theta + \frac{\mathbf{K}\lambda}{L\cos\theta}$$

If we multiply this equation by cosθ we get:

$$\beta_{tot}\cos\theta = \mathbf{C}\varepsilon\sin\theta + \frac{\mathbf{K}\lambda}{L}$$

and comparing this to the standard equation for a straight line (m = slope; c = intercept)

$$y = mx + c$$

we see that by plotting $\beta_{tot}\cos\theta$ versus sinθ we obtain the strain component from the slope ($\mathbf{C}\varepsilon$) and the size component from the intercept ($\mathbf{K}\lambda/L$). Such a plot is known as a Williamson-Hall plot and is illustrated schematically below (note that this plot could alternatively be expressed in reciprocal space parameters, β* versus *d**):

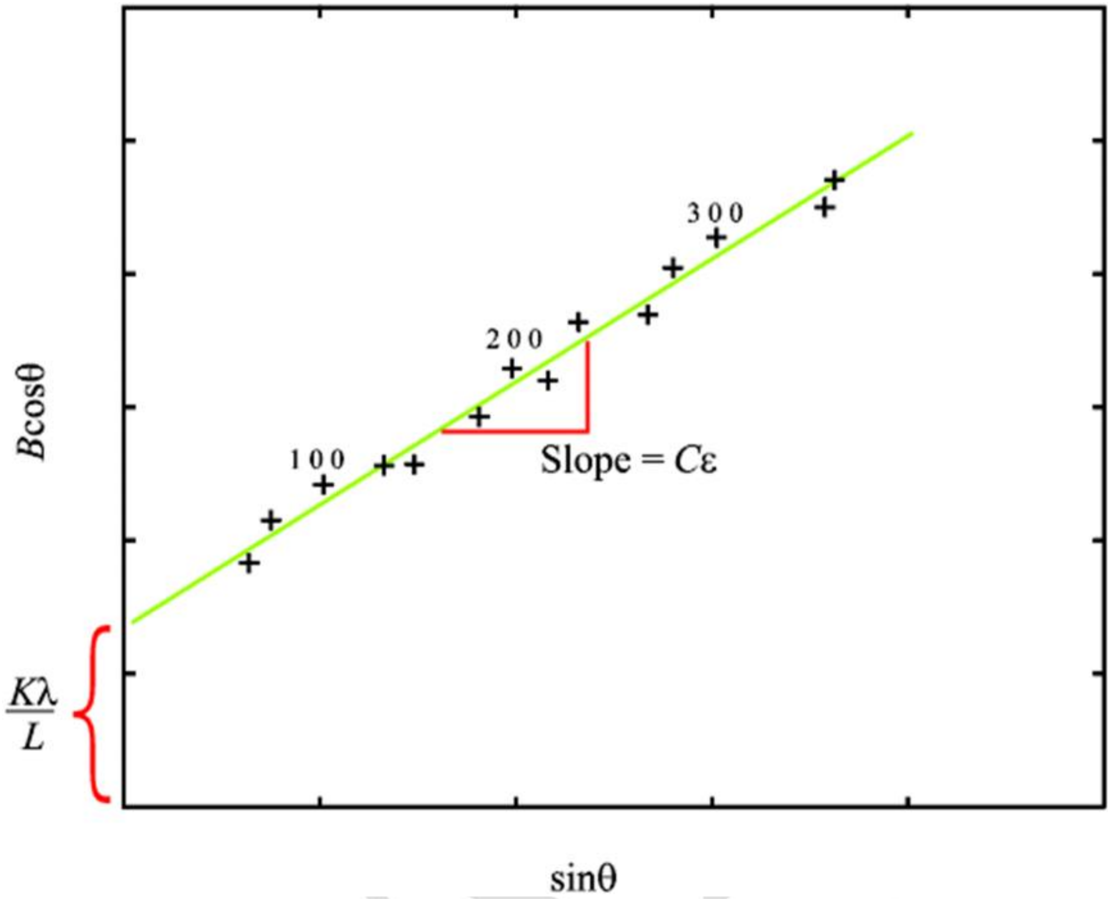

It can be a good idea to label each data point on the Williamson-Hall plot according to the index of its reflection to see whether any pattern emerges: for example, in the illustration several *h*00 reflections seem to lie slightly above the mean straight line suggesting that the powder crystallites are thinnest in the <100> crystal direction. However the Williamson-Hall method has many assumptions: its absolute values should not be taken too seriously but it can be a useful method if used in the relative sense; for example a study of many powder patterns of the same chemical compound, but synthesised under different conditions, might reveal trends in the crystallite size/strain which in turn can be related to the properties of the product.

Warren-Averbach method

This method is attributed to B.E.Warren and B.L.Averbach (J.Appl.Phys. 21, 595(1950) and ibid 23, 497 (1952)) and has become accepted as one of the more rigorous and widely used methods for separating the effects of size and strain. The treatment behind the method is quite complex and involves expressing the peak intensity in terms of a Fourier sum, which has distinct mathematical advantages (half of the terms - the sine components - turn out to be negligible, and (de-)convolution is conveniently handled in Fourier space). A further trick used is to arrange the powder diffraction peaks of a given pattern into *h*,*k*,*l*-indexed groups possessing a common crystallographic direction (e.g. <00*n*> = <001>, <002>, <003> where *n* is referred to as the *order*). This has two particular advantages: it overcomes the problem of asymmetrically sized/strained crystallites as each group analysis then becomes specific for a given direction (i.e. <001> in the above example), and the size/strain separation is simplified by the fact that the size effects are independent of order, *n*, whereas the strain effects vary with order. The method is exact if the strain distribution in the crystallites are Gaussian, and is still a good approximation otherwise provided the crystallite lattice distortions are small. The kind of final values provided by the method are an average (area-weighted) crystallite size, a parameter that is related to the crystallite size distribution and an average strain (for a characteristic size), all specified for a particular crystallographic direction. Even though the method is clearly not straightforward most commercial powder diffractometer systems provide a Warren-Averbach analysis routine on their software with easy-to-follow instructions.

GIXRD and its Applications

X-ray powder diffraction is most widely used for the identification of unknown crystalline materials (e.g. minerals, inorganic compounds). Determination of unknown solids is critical to studies in geology, environmental science, material science, engineering and biology.

Other applications include:

- characterization of crystalline materials
- identification of fine-grained minerals such as clays and mixed layer clays that are difficult to determine optically
- determination of unit cell dimensions
- measurement of sample purity
- With specialized techniques, XRD can be used to:
- determine crystal structures using Riveted refinement
- determine of modal amounts of minerals (quantitative analysis)

- characterize thin films samples by:
    - determining lattice mismatch between film and substrate and to inferring stress and strain
    - determining dislocation density and quality of the film by rocking curve measurements
    - measuring super lattices in multilayered epitaxial structures
    - determining the thickness, roughness and density of the film using glancing incidence X-ray reflectivity measurements
- make textural measurements, such as the orientation of grains, in a polycrystalline sample
- Strengths and Limitations of X-ray Powder Diffraction (XRD)?

Strengths

- Powerful and rapid (< 20 min) technique for identification of an unknown mineral
- In most cases, it provides an unambiguous mineral determination
- Minimal sample preparation is required
- XRD units are widely available
- Data interpretation is relatively straight forward

Limitations

- Homogeneous and single phase material is best for identification of an unknown
- Must have access to a standard reference file of inorganic compounds (d-spacing's, *hul*ls)
- Requires tenths of a gram of material which must be ground into a powder
- For mixed materials, detection limit is ~ 2% of sample
- For unit cell determinations, indexing of patterns for non-isometric crystal systems is complicated
- Peak overlay may occur and worsens for high angle 'reflections'

X-ray Photoelectron Spectroscopy (XPS)

Photoelectron spectroscopy utilizes photo-ionization and analysis of the kinetic energy distribution of the emitted photoelectrons to study the composition and electronic state of the surface region of a sample.

Traditionally, when the technique has been used for surface studies it has been subdivided according to the source of exciting radiation into :

X-ray Photoelectron Spectroscopy (XPS)	- using soft x-rays (with a photon energy of 200-2000 eV) to examine core-levels.
Ultraviolet Photoelectron Spectroscopy (UPS)	- using vacuum UV radiation (with a photon energy of 10-45 eV) to examine valence levels.

The development of synchrotron radiation sources has enabled high resolution studies to be carried out with radiation spanning a much wider and more complete energy range (5 - 5000+ eV) but such work remains a small minority of all photoelectron studies due to the expense, complexity and limited availability of such sources.

Physical Principles

Photoelectron spectroscopy is based upon a single photon in/electron out process and from many viewpoints this underlying process is a much simpler phenomenon than the Auger process.

The energy of a photon of all types of electromagnetic radiation is given by the Einstein relation :

$$E = h\nu$$

Where

h - Planck constant (6.62 x 10^{-34} J s)

ν - frequency (Hz) of the radiation

Photoelectron spectroscopy uses monochromatic sources of radiation (i.e. photons of fixed energy).

In XPS the photon is absorbed by an atom in a molecule or solid, leading to ionization and the emission of a core (inner shell) electron. By contrast, in UPS the photon interacts with valence levels of the molecule or solid, leading to ionisation by removal of one of these valence electrons.

The kinetic energy distribution of the emitted photoelectrons (i.e. the number of emitted photoelectrons as a function of their kinetic energy) can be measured using any appropriate electron energy analyser and a photoelectron spectrum can thus be recorded.

The process of photoionization can be considered in several ways : one way is to look at the overall process as follows :

$$\mathbf{A} + h\nu \rightarrow \mathbf{A}^{+} + \mathbf{e}^{-}$$

Conservation of energy then requires that :

$$\mathbf{E(A)} + h\nu = \mathbf{E(A^{+}) + E(e^{-})}$$

Since the electron's energy is present solely as kinetic energy (KE) this can be rearranged to give the following expression for the KE of the photoelectron:

$$\mathbf{KE} = h\nu - \mathbf{(\,E(A^{+}) - E(A)\,)}$$

The final term in brackets, representing the difference in energy between the ionized and neutral atoms, is generally called the *binding energy* (BE) of the electron - this then leads to the following commonly quoted equation :

$$\mathbf{KE} = h\nu - \mathbf{BE}$$

An alternative approach is to consider a one-electron model along the lines of the following pictorial representation ; this model of the process has the benefit of simplicity but it can be rather misleading.

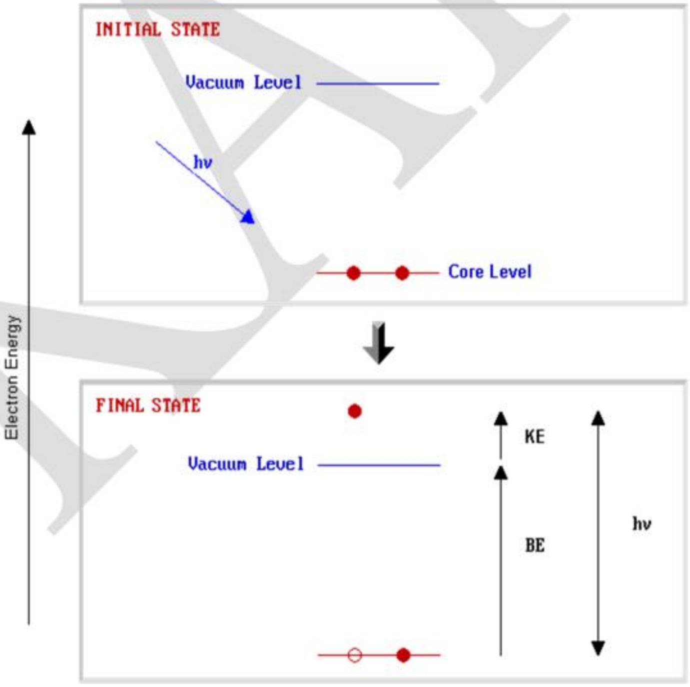

The BE is now taken to be a direct measure of the energy required to just remove the electron concerned from its initial level to the vacuum level and the KE of the photoelectron is again given by :

$$\mathbf{KE = h\nu - BE}$$

NOTE - the binding energies (BE) of energy levels in solids are conventionally measured with respect to the Fermi-level of the solid, rather than the vacuum level. This involves a small correction to the equation given above in order to account for the *work function* (φ) of the solid, but for the purposes of the discussion below this correction will be neglected.

Experimental Details

The basic requirements for a photoemission experiment (XPS or UPS) are:

1. a source of fixed-energy radiation (an x-ray source for XPS or, typically, a He discharge lamp for UPS)

2. an electron energy analyser (which can disperse the emitted electrons according to their kinetic energy, and thereby measure the flux of emitted electrons of a particular energy)

3. a high vacuum environment (to enable the emitted photoelectrons to be analysed without interference from gas phase collisions)

Such a system is illustrated schematically below:

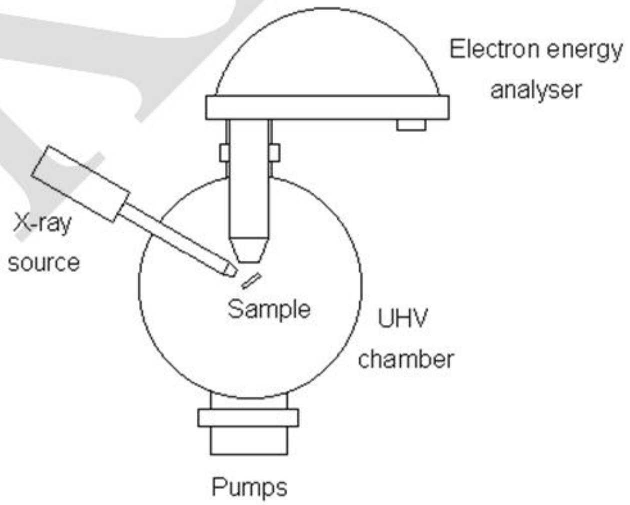

There are many different designs of electron energy analyser but the preferred option for photoemission experiments is a concentric hemispherical analyser (CHA) which uses an electric field between two hemispherical surfaces to disperse the electrons according to their kinetic energy.

X-ray Photoelectron Spectroscopy (XPS)

For each and every element, there will be a characteristic binding energy associated with each core atomic orbital i.e. each element will give rise to a characteristic set of peaks in the hotoelectron spectrum at kinetic energies determined by the photon energy and the respective binding energies. The presence of peaks at particular energies therefore indicates the presence of a specific element in the sample under study - furthermore, the intensity of the peaks is related to the concentration of the element within the sampled region. Thus, the technique provides a *quantitative analysis of the surface composition* and is sometimes known by the alternative acronym, ESCA (Electron Spectroscopy for Chemical Analysis).

The most commonly employed x-ray sources are those giving rise to :

Mg K_α radiation : $h\nu = 1253.6$ eV Al K_α radiation : $h\nu = 1486.6$ eV

The emitted photoelectrons will therefore have kinetic energies in the range of *ca.* 0 - 1250 eV or 0 - 1480 eV . Since such electrons have very short IMFPs in solids, the technique is necessarily surface sensitive.

Example 1 - the XPS spectrum of Pd metal

The diagram below shows a real XPS spectrum obtained from a Pd metal sample using Mg K_α radiation

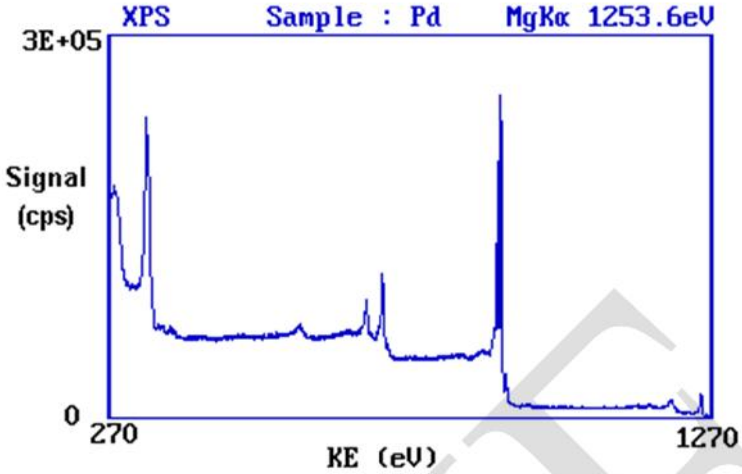

- the main peaks occur at kinetic energies of ca. 330, 690, 720, 910 and 920 eV.

Since the photon energy of the radiation is always known it is a trivial matter to transform the spectrum so that it is plotted against BE as opposed to KE.

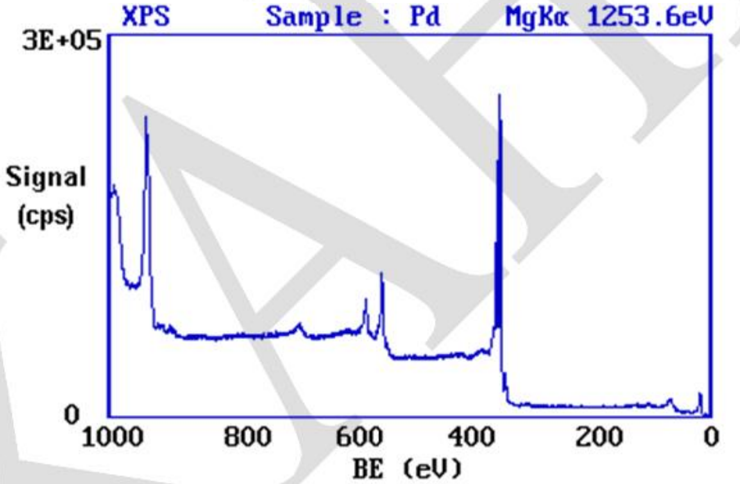

The most intense peak is now seen to occur at a binding energy of ca. 335 eV

Working downwards from the highest energy levels ......

1. the valence band (4*d*, 5*s*) emission occurs at a binding energy of *ca.* 0 - 8 eV (measured with respect to the Fermi level, or alternatively at ca. 4 - 12 eV if measured with respect to the vacuum level).
2. the emission from the 4*p* and 4*s* levels gives rise to very weak peaks at 54 eV and 88 eV respectively

3. the most intense peak at ca. 335 eV is due to emission from the 3*d* levels of the Pd atoms, whilst the 3*p* and 3*s* levels give rise to the peaks at ca. 534/561 eV and 673 eV respectively.
4. the remaining peak is not an XPS peak at all ! - it is an Auger peak arising from x-ray induced Auger emission. It occurs at a kinetic energy of ca. 330 eV (in this case it is really meaningless to refer to an associated binding energy).

These assignments are summarised below

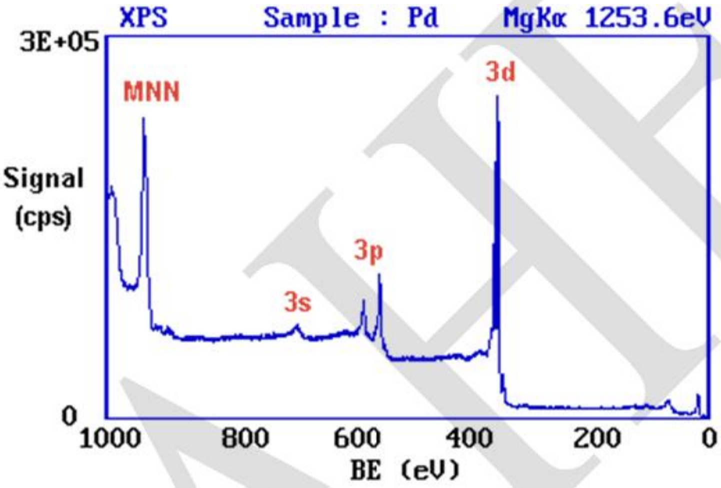

It may be further noted that

- there are significant differences in the natural widths of the various photoemission peaks
- the peak intensities are not simply related to the electron occupancy of the orbitals

Exercise 1 - the XPS spectrum of NaCl

The diagram opposite shows an energy level diagram for sodium with approximate binding energies for the core levels.

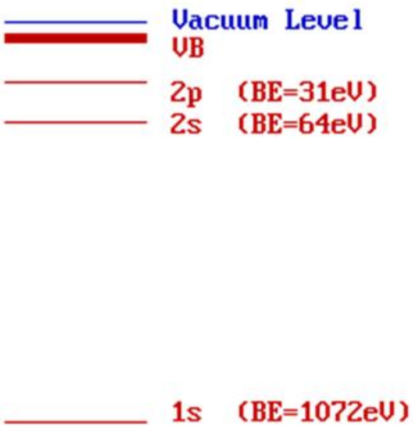

If we are using Mg K_α (*hv* = 1253.6 eV) radiation ...

... at what kinetic energy will the Na 1s photoelectron peak be observed ?

(the 1*s* peak is that resulting from photoionisation of the 1*s* level)

? ... at what kinetic energy will the Na 2s and 2p photoelectron peaks be observed ?

Spin-Orbit Splitting

Closer inspection of the spectrum shows that emission from some levels (most obviously 3*p* and 3*d*) does not give rise to a single photoemission peak, but a closely spaced doublet.

We can see this more clearly if, for example, we expand the spectrum in the region of the 3*d* emission ...

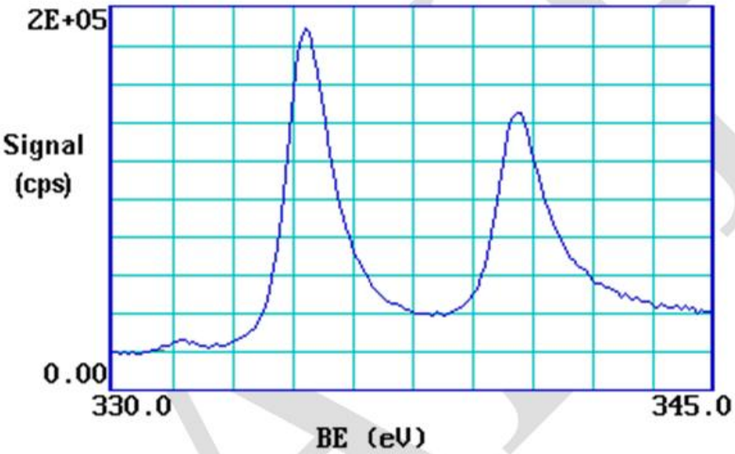

The 3*d* photoemission is in fact split between two peaks, one at 334.9 eV BE and the other at 340.2 eV BE, with an intensity ratio of 3:2 . This arises from spin-orbit coupling effects in the final state.

The inner core electronic configuration of the initial state of the Pd is :

$(1s)^2\ (2s)^2\ (2p)^6\ (3s)^2\ (3p)^6\ (3d)^{10}$ ....

with all sub-shells completely full.

The removal of an electron from the 3*d* sub-shell by photo-ionization leads to a $(3d)^9$ configuration for the final state - since the *d*-orbitals ($l = 2$) have non-zero orbital angular momentum, there will be coupling between the unpaired spin and orbital angular momenta.

Spin-orbit coupling is generally treated using one of two models which correspond to the two limiting ways in which the coupling can occur - these being the *LS* (or Russell-Saunders) coupling approximation and the *j-j* coupling approximation.

If we consider the final ionised state of Pd within the Russell-Saunders coupling approximation, the $(3d)^9$ configuration gives rise to two states (ignoring any coupling with valence levels) which differ slightly in energy and in their degeneracy ...

$^{2D}{}_{5/2}$ $g_J = 2x\{5/2\}+1 = 6$

$^{2D}{}_{3/2}$ $g_J = 2x\{3/2\}+1 = 4$

These two states arise from the coupling of the $L = 2$ and $S = 1/2$ vectors to give permitted J values of 3/2 and 5/2. The lowest energy final state is the one with maximum J (since the shell is more than half-full), i.e. $J = 5/2$, hence this gives rise to the "lower binding energy" peak. The relative intensities of the two peaks reflects the degeneracies of the final states ($g_J = 2J + 1$), which in turn determines the probability of transition to such a state during photoionization.

The Russell-Saunders coupling approximation is best applied only to light atoms and this splitting can alternatively be described using individual electron *l*-*s* coupling. In this case the resultant angular momenta arise from the single hole in the *d*-shell; a *d*-shell electron (or hole) has $l = 2$ and $s = 1/2$, which again gives permitted *j*-values of 3/2 and 5/2 with the latter being lower in energy.

The peaks themselves are conventionally annotated as indicated - note the use of lower case lettering

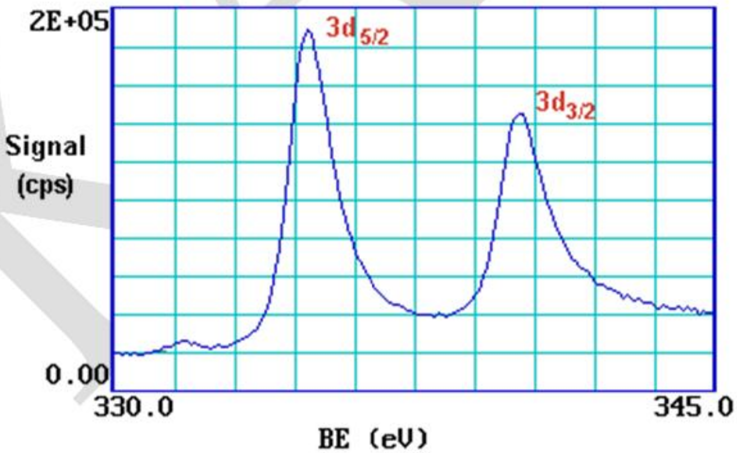

This spin-orbit splitting is of course not evident with *s*-levels ($l = 0$), but is seen with *p*,*d* & *f* core-levels which all show characteristic spin-orbit doublets.

Chemical Shifts

The exact binding energy of an electron depends not only upon the level from which photoemission is occurring, but also upon :

1. the formal oxidation state of the atom
2. the local chemical and physical environment

Changes in either (1) or (2) give rise to small shifts in the peak positions in the spectrum - so-called *chemical shifts* .

Such shifts are readily observable and interpretable in XP spectra (unlike in Auger spectra) because the technique :

- is of high intrinsic resolution (as core levels are discrete and generally of a well-defined energy)
- is a one electron process (thus simplifying the interpretation)

Atoms of a higher positive oxidation state exhibit a higher binding energy due to the extra coulombic interaction between the photo-emitted electron and the ion core. *This ability to discriminate between different oxidation states and chemical environments is one of the major strengths of the XPS technique.*

In practice, the ability to resolve between atoms exhibiting slightly different chemical shifts is limited by the peak widths which are governed by a combination of factors ; especially

- the intrinsic width of the initial level and the lifetime of the final state
- the line-width of the incident radiation - which for traditional x-ray sources can only be improved by using x-ray monochromators
- the resolving power of the electron-energy analyser

In most cases, the second factor is the major contribution to the overall line width.

Angle Dependent Studies

the degree of surface sensitivity of an electron-based technique such as XPS may be varied by collecting photoelectrons emitted at different emission angles to the surface plane. This approach may be used to perform non-destructive analysis of the variation of surface composition with depth (with chemical state specificity).

Surface X-Ray Diffraction

fig. 5

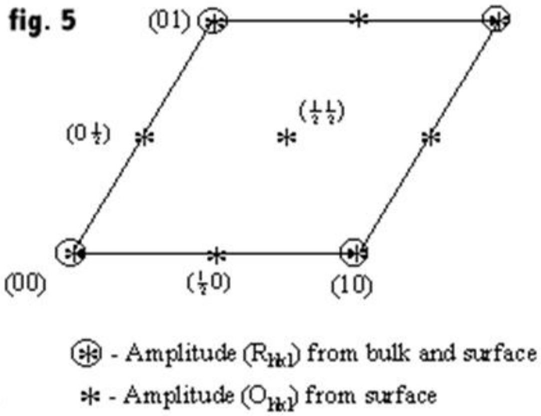

A similar idea allows the direct recovery of surface electron density from measured intensities of reciprocal lattice rods in surface X-ray diffraction. Fig. 5 is a schematic of a diffraction pattern from a (2x2) reconstructed InSb(111) surface. The reciprocal lattice rods run through the Bragg spots on this diagram, and perpendicular to the plane of the figure. It will be noted that the diffraction amplitudes of the integer-order rods are a sum of those from the bulk and surface regions of the sample, while the fractional-order rods arise solely from diffraction from the reconstructed surface region.

The integer-order rods may be treated in a manner entirely analogous to the structure completion problem described in the previous section. The bulk is the known part of the structure and the surface the unknown part. However, inclusion of just the integer-order (crystal truncation) rods alone in the reconstruction algorithm gives only the *average* structure (Fig. 6a) within the surface unit cell (i.e. one which has the bulk 2D periodicity). Nevertheless, this gives an excellent starting electron density for further refinement by inclusion in the algorithm of the fractional-order rod intensities, which finally recovers the accepted vacancy-buckling model [12] in which the Sb atoms in the top double layer closest to the vacancies have moved towards those holes. Such a tendency is apparent even after just 10 iterations of the algorithm following the inclusion of the fractional-order intensities (Fig. 6b). The final reconstructed image (not shown) is even capable of resolving bucklings normal to the surface of as little as 0.2 Å.

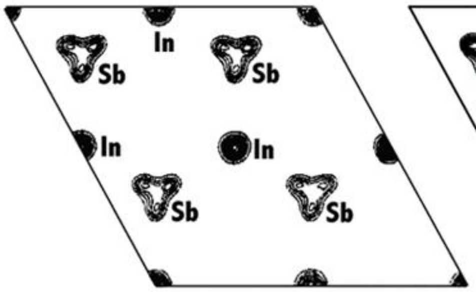

fig. 6a

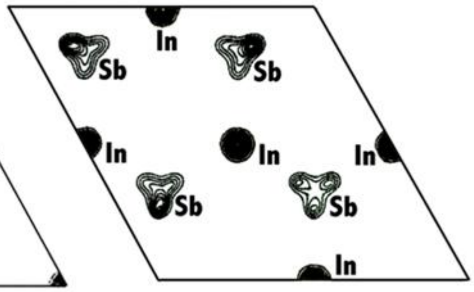

fig. 6b

NEURON DIFFRACTION:

Neutron diffraction or **elastic neutron scattering** is the application of neutron scattering to the determination of the atomic and/or magnetic structure of a material. A sample to be examined is placed in a beam of thermal or cold neutrons to obtain a diffraction pattern that provides information of the structure of the material. The technique is similar to X-ray diffraction but due to their different scattering properties, neutrons and X-rays provide complementary information: X-Rays are suited for superficial analysis, strong x-rays from synchrotron radiation are suited for shallow depths or thin specimens, while neutrons having high penetration depth are suited for bulk samples.

Construction and working of Single Crystal Neutron Diffraction:

The technique requires a source of neutrons. Neutrons are usually produced in a nuclear reactor or spallation source. At a research reactor, other components are needed, including a crystal monochromators, as well as filters to select the desired neutron wavelength. Some parts of the setup may also be movable. At a spallation source, the time of flight technique is used to sort the energies of the incident neutrons (higher energy neutrons are faster), so no monochromatic is needed, but rather a series of aperture elements synchronized to filter neutron pulses with the desired wavelength.

The technique is most commonly performed as powder diffraction, which only requires a polycrystalline powder. Single crystal work is also possible, but the crystals must be much larger than those that are used in single-crystal X-ray crystallography. It is common to use crystals that are about 1 mm^3.

Summarizing, the main disadvantage to neutron diffraction is the requirement for a nuclear reactor. For single crystal work, the technique requires relatively large crystals, which are usually challenging to grow. The advantages to the technique are many - sensitivity to light atoms, ability to distinguish isotopes, absence of radiation damage, as well as a penetration depth of several cm.

Nuclear Scattering:

Like all quantum particles, neutrons can exhibit wave phenomena typically associated with light or sound. Diffraction is one of these phenomena; it occurs when waves encounter obstacles whose size is comparable with the wavelength. If the wavelength of a quantum particle is short enough, atoms or their nuclei can serve as diffraction obstacles. When a beam of neutrons emanating from a reactor is slowed down and selected properly by their speed, their wavelength lies near one angstrom (0.1 nanometer), and the typical separation between atoms in a solid material. Such a beam can then be used to perform a diffraction experiment. Impinging on a crystalline sample, it will scatter under a limited number of well-defined angles, according to the same Bragg's law that describes X-ray diffraction.

Neutrons and X-rays interact with matter differently. X-rays interact primarily with the electron cloud surrounding each atom. The contribution to the diffracted x-ray intensity is therefore larger for atoms with larger atomic number (Z). On the other hand, neutrons interact directly with the *nucleus* of the atom, and the contribution to the diffracted intensity depends on each isotope; for example, regular hydrogen and deuterium contribute differently. It is also often the case that light (low Z) atoms contribute strongly to the diffracted intensity, even in the presence of large Z atoms. The scattering length varies from isotope to isotope rather than linearly with the atomic number. An element like vanadium is a strong scattered of X-rays, but its nuclei hardly scatter neutrons, which is why it is often used as a container material. Non-magnetic neutron diffraction is directly sensitive to the positions of the nuclei of the atoms.

Unlike X-rays, neutrons scatter mostly from the nuclei of the atoms, which are tiny. Furthermore, there is no need for an atomic form factor to describe the shape of the electron cloud of the atom and the scattering power of an atom does not fall off with the scattering angle as it does for X-rays. Diffract grams therefore can show strong well defined diffraction peaks even at high angles, particularly if the experiment is done at low temperatures. Many neutron sources are equipped with liquid helium cooling systems that allow data collection at temperatures down to 4.2 K. The superb high angle (i.e. high *resolution*) information means that the atomic positions in the structure can be determined with high precision. On the other hand, Fourier maps (and to a lesser extent difference Fourier maps) derived from neutron data suffer from series termination errors, sometimes so much that the results are meaningless.

KARPAGAM ACADEMY OF HIGHER EDUCATION, COIMBATORE-21
DEPARTMENT OF PHYSICS
CLASS : I M.SC PHYSICS
BATCH: 2018-2020
PART A : MULTIPLE CHOICE QUESTIONS (ONLINE EXAMINATIONS)
SUBJECT : MATERIAL CHARACTERIZATION
SUBJECT CODE : 18PHP105A
UNIT-I

SL.NO.	QUESTIONS	opt 1	opt2	opt3	opt4	Answer
1	Thin film may be arbitrarily defined as a solid layer having a thickness varying from a few Å to about	10mm	10cm	10µm	10^-3 nm	10µm
2	Thickness of ultra thin film is	>1000Å	50-100Å	100-1000Å	none of these	50-100Å
3	An ideal film extended infinitly in ……………… directions but restricted along………..	two and z direction	one and z direction	three and none	none of these	two and z direction
4	Highly conducting Na, K,Au and Pt etc in the bulk form show -ve TCR when in thin film states thus behaving as	semiconductors	conductors	insulators	dielectrics	semiconductors
5	A freshly formed film surface becomes highly reactive due to	high volume to surface ratio	high surface to volume ratio	high thickness	none of these	high surface to volume ratio
6	Characteristic of a surface are more often observed in ……….	amorphous	single crystal	polycrystalline	thin films	thin films
7	Thin films can be prepared from a variety of materials such as	metals	semiconductors	insulators	all the above	all the above
8	The primary requirement for the methods (a) Thermal deposition and Sputtering is a	high vacuum	higher than ambient pressure	ambient pressure	none of these	high vacuum
9	…………involves the evaporation or sublimation of the material in vacuo by thermal energy	sputtering	CVD	Thermal deposition	chemical deposition	Thermal deposition
10	When all the molecules are condensed, sticking coefficient has a max. value of …………	100	1	10	1000	1
11	When none is deposited, sticking coefficient has a min. value of ………….	1	10	0	-1	0
12	velocity distribution of evaporant molecules will depend on the ………..	nature of the source	nature of the substrate	nature of the target	none of these	nature of the source
13	The emitted vapour stream will have the same velocity distribution in all directions thus resembling the emission from	surface source	point source	cylindrical source	prism source	point source
14	For………………,the emission velocity of the vapour stream will decrease with the increase of the angle of inclination	point source	surface source	cylindrical source	none of these	surface source
15	If Ψ=0, then a surface source resembles a	cylindrical source	point source	cylindrical as well as point source	none of these	point source
16	Heating sources are made from………….	refractory metals	semiconductors	insulators	none of these	refractory metals
17	The amount of deposits received by a substrate will depend not only on the nature of the source but also on the inclination of the vapour stream with the	substrate-normal direction	source-normal direction	source as well as substrate normal	none of these	substrate-normal direction
18	Positioning of the substrate with respect to the source as well as the nature of the source considerably affects the	film growth	film thickness	film purity	none of these	film thickness
19	A high……….generally improves the physical characteristics of the deposited films	source temperature	substrate temperature	nature of the substrate	substrate thickness	substrate temperature
20	Higher vapour pressure constituent will tend to vaporise at a…………..	lower temperature	higher temperature	lower as well as higher temperature	none of these	lower temperature
21	There is no accumulation of the charge on the heated boat in …………	Thermal evaporation	Electron beam method	sputtering	Flash evaporation	Flash evaporation
22	Which method is generally adopted when a material has a tendency to decompose or dissociate during evaporation	Flash evaporation	Electron beam method	sputtering	CVD	Flash evaporation
23	A constant composition film can be produced by ……….	Electron beam method	sputtering	Flash evaporation	CVD	Flash evaporation
24	In which method several sources are simultaneously used for the evaporation of the constituent species	multi evaporation process	Electron beam method	sputtering	evaporation process	multi evaporation process
25	The simultaneous deposition process from different sources is known as ………..	co-evaporation	multi evaporation process	evaporation process	Electron beam method	co-evaporation
26	In electron beam method the electron beam is accelerated with …………..voltage	2V	4kV	10V	2-10kV	2-10kV
27	Which method is now routinely used for the production of metal film resistors and others	Electron beam method	multi evaporation process	sputtering	Flash evaporation	Electron beam method
28	There are ………types of electron beam guns	three	two	one	five	three
29	In …………, electrons are emitted from hair pin type of filament	work accelerated gun	self-accelerated gun	bent beam electron gun	none of these	self-accelerated gun
30	In…………. Electron beam is bent by an appropriate magnetic field	work accelerated gun	self-accelerated gun	bent beam electron gun	none of these	bent beam electron gun
31	The deposition of metal films by sputtering from a cathode by the glow discharge method was first observed by	Wehner	buckel and hilsch	grove	pease	grove
32	Sputtering yield increases with the ……………… of the bombarding ions	mass	energy	mass and energy	none of these	mass and energy
33	Auger transition takes place along with emission of	α-electrons	β-electrons	γ-electrons	radiation less	γ-electrons
34	If the process does not involve any chemical reaction between bombarding gas ions and the cathode is known as	reactive sputtering	physical sputtering	high pressure sputtering	both b and c	both b and c
35	If the process involve any chemical reaction between bombarding gas ions and the cathode is known as	reactive sputtering	physical sputtering	high pressure sputtering	both a and c	both a and c
36	Glow discharge is used to clean ………	dirt	plastics	polymers	none of these	dirt
37	The simplest method of sputtering is by the …………	glow discharge technique	Electron beam method	Flash evaporation	evaporation process	glow discharge technique
38	The minimum voltage at which breakdown takes place is called ………..	transition region	abnormal glow discharge	break down voltage	normal glow discharge	break down voltage
39	In glow discharge sputtering, the region where there is a large increase in voltage as well as current is called the	abnormal glow region	townsend region	normal glow discharge	transition region	abnormal glow region
40	In glow discharge sputtering, the region where there is a large increase in current at a constant voltage is called the	abnormal glow region	townsend region	normal glow discharge	transition region	townsend region

41	A continuous sputtering can take place only in ………….	transition region	townsend region	normal glow discharge	abnormal glow region	abnormal glow region
42	in glow discharge sputtering, luminosity of the…………… is the most intense	cathode glow	negative glow	anode glow	faraday dark space	negative glow
43	Which technique is particularly suitable for refractory materials whicb caannot easily be deposited by other methods	glow discharge sputtering	Electron beam method	Flash evaporation	evaporation process	glow discharge sputtering
44	In…………… method, gases like oxygen or nitrogen are used as media	glow discharge sputtering	Electron beam method	Flash evaporation	reactive sputtering	reactive sputtering
45	Different types of films of mixed compositions can be prepared comparatively easily by	Low pressure sputtering	reactive sputtering	Electron beam method	glow discharge sputtering	reactive sputtering
46	Enhanced ionisation can be achieved in the ………….	r.f.field	d.c.voltage	reactive sputtering	low pressure sputtering	r.f.field
47	Sputtering of cathode materials in presence of inert or active gases either at……….	low pressure	medium pressure	high pressure	all the above	high pressue
48	In low pressure sputtering, ionisation of gas molecules takes place at low vacuum say……….	10^-1 torr	10^-15 torr	10^-10 torr	10^-6 torr	10^-1
49	In RF sputtering method an impedance matching between _________ is necessary	Power supply and electrode	Discharge tube and DC voltage	Power supply and discharge tube	Electrodes and DC voltage	Power supply and discharge tube
50	RF sputtering technique is particularly useful for the deposition of _________.	Insulator	Dielectrics	Semiconductor	Conductor	Dielectrics
51	The deposition of films from gaseous phases by thermal decomposition is known as……….	chemical vapour deposition	sputtering	Thermal deposition	evaporation process	chemical vapour deposition
52	Which technique is used for the preparation of various inorganic as well as organic compounds	chemical vapour deposition	sputtering	Thermal deposition	evaporation process	chemical vapour deposition
53	When tetra ethoxy silane is heated to a temperature of about 700-900°C, a dielectric film of …….is formed	SiO2	Si	SiH4	C	SiO2
54	Gunther method has been used for the preparation of …………… wafers of CdS,CdSe etc.	Single crystal	Polycrystal	Amorphous	both a and c	Single crystal
55	Which method has three temperature zones………	Vapour phase reaction	vapour transportation method	Disproportionation method	pyrolysis	vapour transportation method
56	The SiO2 films can be produced by the reaction of SiCl4 vapours with CO2 in the presence of H2 gas is known as	Gunther method	Philips process	Disproportionation method	pyrolysis	Philips process
57	Which technique is often used for the preparation of very thick films and wafers and even flat shaped crystals of several mm sizes	Vapour phase reaction	vapour transportation method	Disproportionation method	pyrolysis	vapour transportation method
58	Which method depends on the difference in the stability of polyvalent metal compounds at two temperatures	Vapour phase reaction	vapour transportation method	Disproportionation method	pyrolysis	Disproportionation method
59	Which method depends on the deposition of films from aqueous solutions either by passing a current or by chemical reactions	chemical deposition	chemical vapour deposition	evaporation process	sputtering	chemical deposition
60	In …………… process metal films can be deposited without passing any current	electrodeposition	anodic oxidation	electroless plating	chemical reaction	electroless plating
61	In mass method balance methods is made of……….	silica	glass	quartz	magnesium	quartz
62	In crystal oscillator thickness measurement depends on the oscillation of a	Quartz fibre	Quartz crystal	Quartz amorphous	Quartz film	Quartz crystal
63	Which method uses interference fringes for the measurement of film thickness?	crystal oscillator	photometric	ellipsometry	interferometry	interferometry
64	Which of the following technique comes under mass methods	crystal oscillator	photometric	ellipsometry	interferometry	crystal oscillator
65	Which is a very accurate method which is eminently suitable for measuring the thickness of surface layers or films as well as their optical constants	ellipsometry	interferometry	photometric	microbalance	ellipsometry
66	Degreasing and cleaning are carried out in a closed chamber by suspending the substrates in vapours of organic solvents such as	carbon tetrachloride	alcohol	trichloro ethylene	both a and c	both a and c

SYLLABUS

Thermal Analysis

Introduction - Definitions, Codes of Practice and Nomenclature - thermogravimetric analysis (TGA) - instrumentation - determination of weight loss and decomposition products - differential thermal analysis (DTA) - cooling curves - differential scanning calorimetry (DSC) - instrumentation - specific heat capacity measurements - determination of thermomechanical parameters .

THERMAL ANALYSIS

Thermal analysis is a branch of materials science where the properties of materials are studied as they change with temperature. Several methods are commonly used – these are distinguished from one another by the property which is measured:

- Dielectric thermal analysis (DEA): dielectric permittivity and loss factor
- Differential thermal analysis (DTA): temperature difference versus temperature or time
- Differential scanning calorimetric (DSC): heat flow changes versus temperature or time
- Dilatometer (DIL): volume changes with temperature change
- Dynamic mechanical analysis (DMA or DMTA) : measures storage modulus (stiffness) and loss modulus (damping) versus temperature, time and frequency
- Evolved gas analysis (EGA): analysis of gases evolved during heating of a material, usually decomposition products
- Laser flash analysis (LFA): thermal diffusivity and thermal conductivity
- Thermo gravimetric analysis (TGA): mass change versus temperature or time
- Thermo mechanical analysis (TMA): dimensional changes versus temperature or time
- Thermo-optical analysis (TOA): optical properties
- Derivatography: A complex method in thermal analysis[1]

Simultaneous thermal analysis (STA) generally refers to the simultaneous application of thermogravimetry (TGA) and differential scanning calorimetric (DSC) to one and the same sample in a single instrument. The test conditions are perfectly identical for the TGA and DSC signals (same atmosphere, gas flow rate, vapor pressure of the sample, heating rate, thermal contact to the sample crucible and sensor, radiation effect, etc.). The information gathered can even be enhanced by coupling the STA instrument to an Evolved Gas Analyzer (EGA) like Fourier transform infrared spectroscopy (FTIR) or mass spectrometry (MS).

Other, less common, methods measure the sound or light emission from a sample, or the electrical discharge from a dielectric material, or the mechanical relaxation in a stressed specimen. The essence of all these techniques is that the sample's response is recorded as a function of temperature (and time).

It is usual to control the temperature in a predetermined way - either by a continuous increase or decrease in temperature at a constant rate (linear heating/cooling) or by carrying out a series of determinations at different temperatures (stepwise isothermal measurements). More advanced temperature profiles have been developed which use an oscillating (usually sine or square wave) heating rate (Modulated Temperature Thermal Analysis) or modify the heating rate in response to changes in the system's properties (Sample Controlled Thermal Analysis).

In addition to controlling the temperature of the sample, it is also important to control its environment (e.g. atmosphere). Measurements may be carried out in air or under an inert gas (e.g. nitrogen or helium). Reducing or reactive atmospheres have also been used and measurements are even carried out with the sample surrounded by water or other liquids. Inverse gas chromatography is a technique which studies the interaction of gases and vapors with a surface - measurements are often made at different temperatures so that these experiments can be considered to come under the auspices of Thermal Analysis.

Atomic force microscopy uses a fine stylus to map the topography and mechanical properties of surfaces to high spatial resolution. By controlling the temperature of the heated tip and/or the sample a form of spatially resolved thermal analysis can be carried out.

Thermal analysis is also often used as a term for the study of transfer through structures. Many of the basic engineering data for modelling such systems comes from measurements of heat capacity and thermal conductivity.

The thermal analysis is one of the important and oldest methods to analyze the thermal behavior of the materials. Sophisticated instruments have been developed to get useful quantitative and qualitative information on the desired materials with respect to temperature change. The advanced thermal analysis instruments are used to measure various properties such as weight loss, phase transformation, glass transition, specific heat capacity, the energy of enthalpy, thermomechanical behavior, viscoelastic properties and reaction kinetics (Michael 2004).

1.7.5.1 Thermogravimetric analysis

Thermogravimetric analysis (TGA) measures the rate of change in mass of the sample as the function of temperature or time under controlled atmosphere. TGA is widely used to identify the oxidation, thermal stability and volatility properties of samples. Thermobalance consists of a programmable temperature controller with a computer and an electronic microbalance with the furnace which controls the temperature and simultaneously measures the heating or cooling temperature and weight of the sample. The three important thermogram signals are collected when analyzing the samples, which are, temperature, weight and rate of weight change (i.e., differential thermogravimetric). The loss of mass is recorded with respect to temperature or time. Owing to the nature of the bond between molecules, the mass loss percentage is varied when increasing the temperature. The schematic diagram of TG analyzer is shown in Figure 1.7.

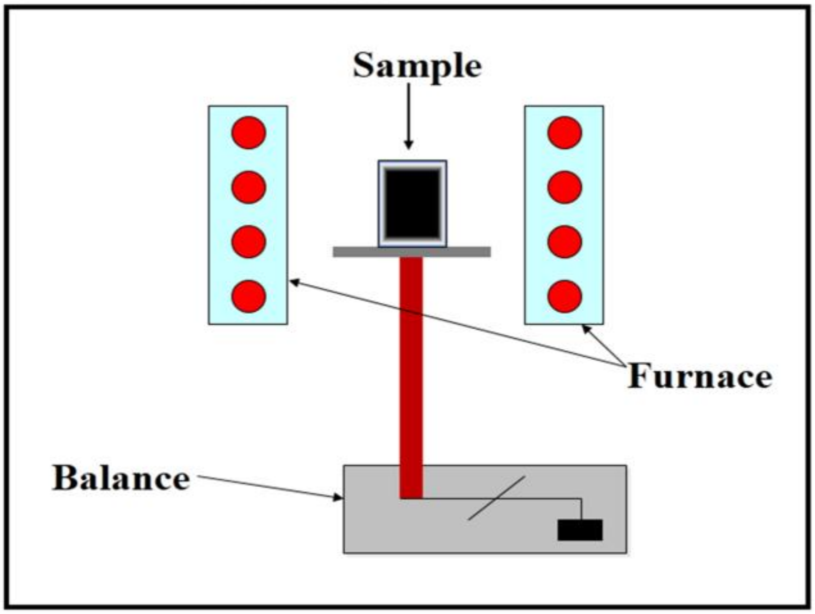

Figure 1.7 The schematic diagram of TG analyzer

Thermogravimetry provides a quantitative measurement of any weight changes associated with thermally induced transitions. For example TG can record directly the loss in weight as a function of temperature or time for transitions that involves dehydration or decomposition. The rates of these thermally induced processes are often a function of the molecular structure charges in weight result from physical and chemical bonds forming and breaking at elevated temperature. TG data are useful in characterizing materials as well as in investigating the thermodynamics and kinetics of the reaction and transitions that result from the application of heat to these materials. The usual temperature range for TG is from ambient to 1200 °c in either inert or reaction atmosphere.

Instrumentation

In TG the weight of the sample is continuously recorded as the temperature is increased. Samples are placed in a crucible or shallow discs that is positioned in a furnace on a quartz beam attached to an automatic recording balance. TG instrument that contains a taut- ban suspension electromechanical transducer. The horizontal quartz beam is maintained in the null position by the current flowing through the transducer coil of an electromagnetic balance. A pair of photo sensitive diodes acts as a position sensor to determine the movement of the beam. Any change in the weight of the sample causes a deflection of the beam, which is sensed by one of the photo diodes. The beam is then restored to the original null position by a feedback current sent from the photo diodes to the coil of the balance.

TG curve

The weight change TG curve can be understood by using the curve for a single component and binary mixtures. The crucible is removed from the thermo balance then it is cleaned and dried and again put in position in the thermo balance. Then, thermo balance is operated to get a base line which is indicated by dash line. The substance to be determined is precipitated by a suitable precipitant and then transferred to the crucible. Now the heating in the thermo balance is started and the weight loss curve is recorded as usual to get the thermo gram.

Application

i) TG is useful to determine the correct drying temperatures of precipitates.
ii) TG is useful to find suitable standards in analytical chemistry.
iii) Thermo balance study can be used in determining the purity of various substances.
iv) TG can also be used to study the thermal effects on induced magnetism and evaluating the effects of heat on ferromagnetic materials.
v) TG has been used to study the reaction between certain oxides.

DIFFERENTIAL THERMAL ANALYSIS

In differential thermal analysis (DTA), the temperature difference between the inert reference and a test sample is measured and recorded. The furnace is heated under defined atmospheric condition. The variation of heat absorption or desorption of the sample is compared with an inert reference sample. From DTA instruments the thermal properties and phase variation of the sample can be identified but this method cannot quantify the enthalpy change. Low heating rate and sample weight lead sharper peak of high resolution which also influences the properties of decomposition phenomenon and kinetics. In the case of single-component systems, only simple phase transformation occurs. For multiple components, many phases such as formation and deformation of materials can be noticed.

Differential thermal analysis (DTA) technique is simple as it involves the technique of recording the difference in temperature between a substance and a reference material against either time or temperature as the two specimens are subjected to identical temperature in an environment heated or cooled at a controlled rate. Thus a differential thermo gram consists of a record of the difference in sample and reference temperature (differential temperature ΔT) plotted as a function of time 't', sample temperature (T_s), reference temperature (T_r) or furnace temperature (T_f).

Instrumentation

A large number of different types of instruments are available for DTA studies. However a typical DTA apparatus is shown. The various components of a DTA apparatus are as follows

Furnace

This is a device for heating the sample in the apparatus, one always prefers a tabular furnace. This is constructed with an appropriate material (wire or ribbon) wound on a refractory tube. Such furnace possess the desired characteristics for good temperature regulation and programming these are fairly inexpensive. Generally the choice of the resistance material as well as refractory is decided from the intended maximum temperature of operation and gaseous environments.

Sample holder

This is used to contain the sample as well as the reference material. Generally sample holder made up of platinum is employed. In the most of the DTA instruments, specimen holder assemblies are identical isolated cups supported on thermocouple as well as metallic or nonmetallic blocks with wells. In these assemblies, the sample or the reference material can either be packed in the respective wells, which fit tightly into the wells resulting effectively heat transfer. In these assemblies, the reference temperature may be measured either at the center of reference or sample using the respective arm of the differential thermocouple.

Temperature controller/ sensors

In order to control temperature, the three basic elements are required, they are sensor, control element and heater. The control element governs the rate of heat input required to match the heat loss from the system. The location of the sensor with respect to the heater and made of heat transfer measure the time elapsed between sensing and variation in heat input. It there occurs adjustment between these three components, successful temperature control is possible.

Recorder

This is to record the DTA curve in thermo analytical studies the signals obtained from the sensors can be recorded in which the signal trace is produced on paper or film, by ink, heating stylus, electric writing or optical beam.

DC Amplifier and furnace programmer

In DTA apparatus, generally a low level Dc amplifier is employed and the main function of furnace temperature programmer is to increase the temperature of the furnace at a steady rate.

DTA curve

In the ideal DTA curve there is an exothermic peak and an endothermic peak. Both the shape and size of the peak may furnished good information about the nature of test sample. Generally, sharp endothermic peaks give ideas of change in crystallinity or fusion processes whereas broad end. In most of the cases, physical changes give rise to endothermic curves whereas chemical reactions give rise to exothermic peaks. The origin of the temperature difference in the sample (ΔT) lies in the energy difference between the product and the reactants or between the product and the reactants or between the two phases of a substance. This energy differences is manifested as enthalpic changes either exothermic or endothermic.

Application

i) Fingerprinting by the pattern of thermo grams, qualitative and quantitative analyses by peak area or height for a wide range of materials.

ii) Study of thermal characteristics, stability, degradation and reaction kinetics on small samples, over a temperature range of -175 °C to 1000 °C and above.

DIFFERENTIAL SCANNING CALORIMETRY

Differential scanning calorimetry (DSC) is one of the most important analytical tools in the thermal analysis that measures the flow of heat in the sample and gives the information about the change in physical properties with the function of temperature. The DSC instrument is also similar to DTA apparatus but the electrical energy is used to restore the cooler of the both sample and reference materials. Figure 1.8 illustrate the schematic diagram of DSC apparatus. Depending on nature of sample endothermic or exothermic process occurs during heat flow through the sample. The DSC instrument can be operated in two ways, heating and cooling with constant heating or cooling rate. The schematic (Figure 1.9) representation reveals the possible transitions that are produced from DSC curve but all the parameters could not occur in a single compound or sample.

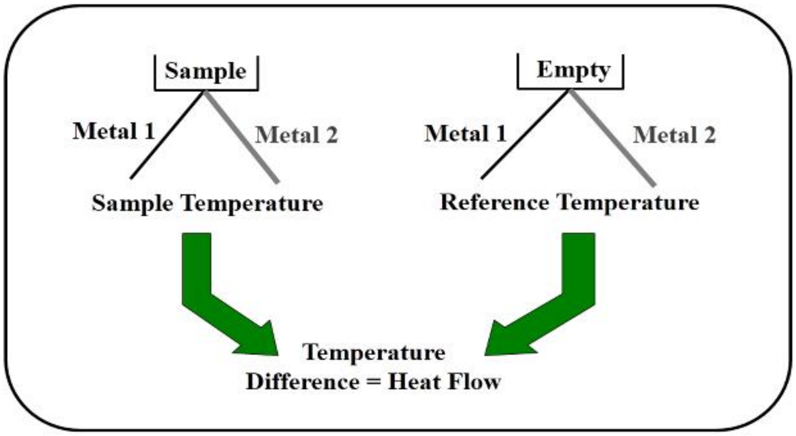

The schematic diagram of DSC apparatus

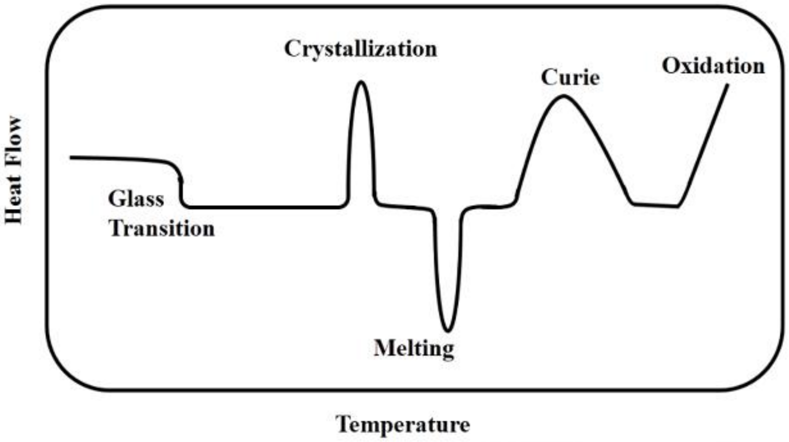

Possible thermal behavior of sample with respect to temperature and heat flow

Thermal kinetics

The thermal parameters of material play an important role in nucleation formation (Cahoon 2012). Thermal kinetics is one of the most important analysis to understand the nucleation mechanism in every crystal growth process. The knowledge about thermal kinetics is useful to grow better quality crystals from melt growth techniques. By using Arrhenius equation, thermal kinetic parameters were calculated for many inorganic glasses and compounds such as hydrated iron sulphate (Straszko et al 1997), dolomite (Olszak-Humienik & Możejko 1999), molybdate (IV) and tungstate (IV) with chromium (III) (Ali & Kowsar 1998) and cobalt sulphate hexahydrate (Straszko et al 2000). Even though there are many characterization and interpretations on organic crystals grown by solution and melt growth methods, only limited investigation reports are available on thermal kinetic parameters of organic materials. The researchers have performed non-isothermal and isothermal studies for various compounds, in which non - isothermal condition is implemented for a wide range of temperature in lesser time duration (Sidel et al 2011). Arrhenius equation is used generally to evaluate the thermal kinetic parameters. However, different types of equations were derived from Arrhenius equation by other researchers like Kissingers (Kissinger & Homer 1957), Ozawa (Ozawa 1970), Augis and Bennet (Augis & Bennett 1978), Kissinger - Akahira - Sunose (KAS) and Ozawa - Flynn - Wall (OFW) (Benavidez et al 2011) to estimate the values of thermal kinetic parameter.

The data conversion from thermogram given by the thermal analysis instrument into kinetic parameters such as activation energy, the order of reaction, rate constant and frequency factor or pre-exponential factor is mainly based on utilization of classical kinetic laws. The rate of chemical reaction ($\frac{d\alpha}{dt}$) is a function of degree of conversion (α) and it is expressed as,

$$\frac{\mathrm{d}\alpha}{\mathrm{dt}} = \mathrm{k.\,f}(\alpha) \qquad (1.2)$$

where, k is the rate constant and α can be evaluated from the thermogravimetric curve of the material.

The classic Kissinger equation is used for the calculation of thermal kinetic parameters from DTA curves. Kinetic parameters and reaction mechanism can be determined simultaneously by generalized Kissinger equation. The Kissingers equation gives an analytical solution, which correlate the kinetic behavior of melting or decomposition peak temperatures. The better results were achieved from Kissinger equation which is due to the consideration of many assumptions in the equation. Hence, the application of Kissinger equation is extended widely. The Kissinger equation is represented as,

$$\ln\left(\frac{\beta}{T_m^2}\right) = \frac{-E_a}{RT_m} + \ln\left(\frac{K_0 R}{E_a}\right) \qquad (1.3)$$

While applying this equation to non - first - order kinetics, similar results are obtained. The activation energy is calculated using isoconversional methods which are a logarithmic form of the kinetic equation. Owing to the repeatability of this calculation method, it is recommended for calculating the activation energy of various materials.

The degree of conversion (α) is the most useful parameter for the calculation of kinetic parameters at single heating rate and it is defined by the relation,

$$\alpha = \frac{M_s - M(t,T)}{M_s - M_f} \qquad (1.4)$$

where, M_s - initial mass, M_f - final mass and M(t,T) - instantaneous mass which depends on temperature and time. The calculated values of α can be substituted in such kinetic equations derived by Coats and Redfern or Friedman methods, the thermal kinetic parameter can be evaluated.

KARPAGAM ACADEMY OF HIGHER EDUCATION, COIMBATORE-21
DEPARTMENT OF PHYSICS
CLASS : I M.SC PHYSICS
BATCH: 2018-2020
PART A : MULTIPLE CHOICE QUESTIONS (ONLINE EXAMINATIONS)
SUBJECT : MATERIAL CHARACTERIZATION
SUBJECT CODE : 18PHP105A
UNIT-II

SL.NO.	QUESTIONS	opt 1	opt2	opt3	opt4	Answer
1	In electron diffraction technique maximum voltage upto ……	60-63keV	60-65eV	60-65keV	60-63eV	60-65keV
2	………Is used to analyse the surface layers of metals, semiconductor and insulators	SEM	LEED	XPS	HEED	XPS
3	The surface layers of Ni single crystal was first made by…….	Davisson	Thomson	germer	both a and b	both a and c
4	In Finch type camera, a maximum voltage is limited upto ………	100keV	200keV	65keV	40keV	65keV
5	In HEED method the accelerating potential of electrons is about ……..	40 to 100keV	60 to 200keV	5 to 500eV	both a and b	both a and b
6	In LEED method the accelerating potential of electrons is about …….	5 to 500eV	60 to 200keV	40 to 100keV	none of these	5 to 500eV
7	For transmission method the material thickness should be lower than ……..	1000Å	500Å	10000Å	13000Å	500Å
8	The vacuum conditions in LEED is in an order of ……..	10^-9 to 10^-10 torr	10^-4 to 10^-6 torr	10^-1 to 10^-2 torr	< 10^-1 torr	10^-9 to 10^-10 torr
9	……..is used as a standard material in HEED	graphite	magnesium	copper	tin	graphite
10	Which method provide information of both surface layers and different layers constituting the material can be	LEED	HEED	SEM	TEM	HEED
11	The function of repeller in LEED …………	cannot passes inelastically scattered electrons	passes inelastically scattered electrons	passes elastically scattered electrons	cannot passes elastically scattered electrons	cannot passes inelastically scattered electrons
12	A LEED concerns primarily about the nature of the ……….	surface layer	surface contamination	formation of oxide layers	all the above	all the above
13	Slow electrons because of their low energy interact…….with matter	weakly	strongly	mediumly	both a and b	strongly
14	The resolution in an electron microscope is sbout……..	5-10Å	<5Å	>5Å	100Å	5-10Å
15	………..is one of the most useful and versatile instruments for the investigation of surface topography, microstructural feature, etc.	scanning electron microscope	LEED	HEED	TEM	scanning electron microscope
16	The secondary electrons have very low energy say…...	<100eV	>100eV	<50eV	60eV	<50eV
17	SEM technique along with…………….. Is widely used for surface studies	Auger electron spectroscopy	electron microprobe	field emission microscopy	both a and b	both a and b
18	The composition of the surface material is readily determined from the……….	positions of the peaks in the spectra	shifts of the ESCA peaks	the shape of the ESCA peaks	all the above	positions of the peaks in the spectra
19	…………is a very useful tool for the analysis of organic compounds and polymer materials of thickness about 40 to 100Å	SEM	LEED	HEED	XPS	XPS
20	In SIMS, the sputtered particles come out as……..	positive ions	negative ions	neutrals	all the above	all the above
21	The condensation of vapour atoms on a neutral solid takes place from a ……………. Condition of vapours	supersaturated	saturated	under saturated	either a or b	supersaturated
22	……………….nucleation involves film formation over a foreign substrate surface	heterogeneous	homogeneous	either a or b	both a and b	heterogeneous
23	If the substrate is of the same material as the vapour atoms then the nucleation process is called ……………	homogeneous	heterogeneous	either a or b	both a and b	homogeneous
24	Formation of critical nucleus involves the …………… of heat of condensation of vapour atoms	release	absorption	adsorption	transfer	release
25	Impinging atoms can be reflected back to vapour state without……………….	evaporation	condensation	absorption	desorption	condensation
26	Evaporation can take place at stages ……………	1,2,3 and 4	1,2,3 and 5	1,2 and 3	1,4 and 5	1,2,3 and 5
27	A higher Ts generally favours a larger grain size due to the increasing ………….of the surface ad-atoms	absorption	adsorption	mobility	condensation	mobility
28	A……….size of area can be examined with mass spectroscopy	micron	nano	cm	mm	micron
29	If the ions have the same energy, the radii of curvatures will be …………	mass	volume	density	size	mass

30	………….is a very sensitive method to identify the elemental composition of a film	mass spectroscopy	SIMS	SEM	XPS	mass spectroscopy
31	Adsorbed species after migration collide to form …………..	subcritical nuclei	critical nuclei	cluster	either a or b or c	either a or b or c
32	In a thermally equilibrated system of impinging atoms, the probability of condensed atoms sticking to the substrate surface is known as……….	thermal accomodation	sticking coefficient	absorption coefficient	either a or b	either a or b
33	…………..is a microscopic and short-lived phase(metastable)	surface-solid phase	surface-liquid phase	surface-gas phase	bulk-gas phase	surface-gas phase
34	Ad-atoms also called ………….	monomers	dimers	trimers	polymers	monomer
35	When thermal equilibrium is established the flux of impinging atoms on the substrate will be equal to the ……………..flux of atoms	re-evaporations	desorbed	adsorbed	either a or b	either a or b
36	The surface diffusion generally takes place by ……………………of an ad-atom from one possible site to a next one	jumping	hopping	moving	either a or b	either a or b
37	The root mean square distance travelled by an ad-atom before ……………………is an important factor in nucleation process	evaporation	desorption	condensation	none of the above	desorption
38	In order to explain the nucleation and cluster formation …………models have been found useful	capillarity	atomistic or statistical models	BCF model	both a and b	both a and b
39	Capillarity Model is an extension of the classical theory of Volmer-Weber-Becker-Doring for …………..of a supersaturated vapour phase to the liquid state	phase transition	adsorption	condensation	none of the above	condensation
40	The surface energy will of course increase with …………….r	increasing	decreasing	constant	either a or b	increasing
41	If a molecular volume of the film material is condensed from a supersaturated vapour pressure to equilibrium pressure of bulk liquid ΔG_v is given by	$-(KT/V)\ln(p/p_e)$	$(KT/V)\ln(p/p_e)$	$(KT)\ln(p/p_e)$	$(KT)\ln(R/R_e)$	$-(KT/V)\ln(p/pe)$
42	For high supersaturations the critical cluster may consist of…………..atom	one	two	three	many	one
43	From critical nuclei of 2 and 3 atoms stable clusters of 3 and 4 atoms in …………. And …………..arrangements respectively are obtained	single and square	triangular and square	square and hexagonal	triangular and hexagonal	triangular and square
44	The formation of these islands and their growth take place either by …………	direct addition of atoms from the vapour phase	from other environment	by the diffusion controlled process of ad-atoms	any of the above	any of the above
45	Islands consist of comparatively larger nuclei say greater than…………	10Å	1Å	10nm	1mm	10Å
46	The ……………..controlled process is more commonly observed except at low substrate temperature	evaporation	diffusion	absorption	desorption	diffusion
47	The smallest stable nuclei are of radii of about …………	10Å	5Å	10cm	1mm	5Å
48	Most embryos prior to the formation of island structure are of sizes about …………..	15-30Å	greater than 30Å	less than 15Å	none of the above	15-30Å
49	An island will be made up about …………atoms or more	50-100	100-200	300-600	10-200	50-100
50	The surface migration distance of ad-atoms of silver deposited from the vapour phase has been estimated to be about………..	500nm	500μm	500Å	300nm	500Å
51	The coalescence involves considerable transfer of ……….. Between island by diffusion	atoms	molecules	mass	volume	mass
52	The time of coalescence is very short say about ………………	0.6second	3second	30second	40second	0.6second
53	with…………film thickness, holes or gaps will decrease in size	increasing	decreasing	constant	none of the above	increasing
54	The minimum film thickness for the continuous stage is also dependent on the ………………	nature of the deposits	modes of deposition	deposition parameters	all the above	all the above
55	The number of………………….. can be reduced by the thermal annealing process	foreign species	impurities	grain boundaries	all the above	grain boundaries
56	Defects such as …………can also develop during nucleations and grain growths	twinning	stacking fault	dislocation	all the above	all the above
57	…………films often develop surface asperities and roughness	thicker	thin	very thick	none of the above	thicker
58	The formation of larger masses of nuclei resulting in the …………. Of the nucleation density	decrease	increase	either a or b	no change	decrease
59	In an electron diffraction camera monochromatic electrons pass through an aperture of a	Diaphragm	Specimen	Focusing coil	Screen	Diaphragm
60	In electron diffraction camera _________ works as the anode normally at the earth potential	Mono chromatic electron beam source	Specimen	Diaphragm	Focusing coil	Diaphragm
61	Electron beam should be _________.	Coherent	Monochromatic	High intense	Both a& b	Both a& b

SYLLABUS

Magnetic Analysis

Vibrating sample magnetometer - SQUID : Introduction - construction and working principle.

Optical Microscopy

Optical microscopy techniques - Bright field - Dark field optical microscopy - phase contrast microscopy -differential interference contrast microscopy - fluorescence microscopy - confocal microscopy - Metallurgical microscope.

VIBRATING-SAMPLE MAGNETOMETER (VSM)

A **vibrating-sample magnetometer** (VSM) is a scientific instrument that measures magnetic properties. Simon Finer at MIT Lincoln Laboratory invented VSM in 1955 and reported it in 1959. A sample is first magnetized in a uniform magnetic field. It is then sinusoidal vibrated, typically through the use of a piezoelectric material. Commercial systems use linear actuators of some form. Historically, these systems were developed using modified audio speakers, though this approach was dropped due to the interference through the produced in-phase magnetic noise, as the magnetic flux through a nearby pickup coil varies sinusoidal. The induced voltage in the pickup coil is proportional to the sample's magnetic moment, but does not depend on the strength of the applied magnetic field. In a typical setup, the induced voltage is measured with an amplifier using the piezoelectric signal as a frequency reference. It is also possible to record the hysteresis curve of a material by sweeping the magnetic field.

The idea of vibrating sample came from D. O. Smith’s vibrating-coil magnetometer.

A schematic drawing of the VSM sample holder and detection mechanism of VSM is shown in Figure 30.01. The set up was invented by Simon Foner at MIT in 1955.

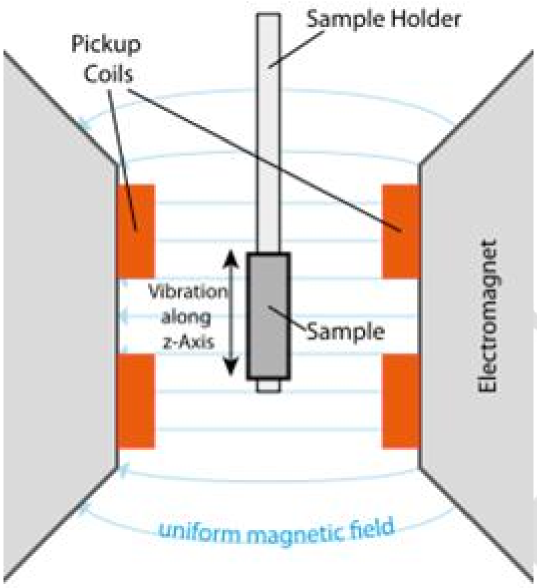

Figure 30.01: Schematic of sample holder and VSM mechanism.

- A sample to be studied is placed inside the uniform magnetic field and then vibrated sinusoidally using vibrator made of linear actuators or modified audio speakers.

- The induced voltage in the pickup coil is proportional to the sample's magnetic moment, but does not depend on the strength of the applied magnetic field.

- In a typical setup, the induced voltage is measured through the lock-in amplifier using the piezoelectric signal as its reference signal. Lock-in principle of measurement allows the measurement of signal weaker than the noise. By measuring in the field of an external electromagnet, it is possible to obtain the hysteresis curve of a material.

- VSM measures the magnetization of a small sample of magnetic material placed in an external magnetizing field by converting the dipole field of the sample into an AC electrical signal.

SQUID

A **SQUID** (for **superconducting quantum interference device**) is a very sensitive magnetometer used to measure extremely subtle magnetic fields, based on superconducting loops containing Josephson junctions.

SQUIDs are sensitive enough to measure fields as low as 5 at (5×10^{-18} T) with a few days of averaged measurements.[1] Their noise levels are as low as 3 $\text{fT}\cdot\text{Hz}^{-1/2}$.[2] For comparison, a typical refrigerator magnet produces 0.01 tesla (10^{-2} T), and some processes in animals produce very small magnetic fields between 10^{-9} T and 10^{-6} T. Recently invented SERF atomic magnetometers are potentially more sensitive and do not require cryogenic refrigeration but are orders of magnitude larger in size (~1 cm^3) and must be operated in a near-zero magnetic field.

Optical microscope,

The **optical microscope**, often referred to as the **light microscope**, is a type of microscope that uses visible light and a system of lenses to magnify images of small subjects. Optical microscopes are the oldest design of microscope and were possibly invented in their present compound form in the 17th century. Basic optical microscopes can be very simple, although many complex designs aim to improve resolution and sample contrast.

The image from an optical microscope can be captured by normal, photosensitive cameras to generate a micrograph. Originally images were captured by photographic film, but modern developments in CMOS and charge-coupled device (CCD) cameras allow the capture of digital images. Purely digital microscopes are now available which use a CCD camera to examine a sample, showing the resulting image directly on a computer screen without the need for eyepieces.

Alternatives to optical microscopy which do not use visible light include scanning electron microscopy and transmission electron microscopy and scanning probe microscopy.

On 8 October 2014, the Nobel Prize in Chemistry was awarded to Eric Bet zig, William Mourner and Stefan Hell for "the development of super-resolved fluorescence microscopy," which brings "optical microscopy into the nan dimension

Types:

There are two basic types of optical microscopes: simple microscopes and compound microscopes. A simple microscope is one which uses a single lens for magnification, such as a magnifying glass. A compound microscope uses several lenses to enhance the magnification of an object. The vast majority of modern research microscopes are compound microscopes while some cheaper commercial digital microscopes are simple single lens microscopes. Compound microscopes can be further divided into a variety of other types of microscopes which differ in their optical configurations, cost, and intended purposes

Simple microscope

A simple microscope uses a lens or set of lenses to enlarge an object through angular magnification alone, giving the viewer an erect enlarged virtual image.[3][4] The use of a single convex lens or groups of lenses are found in simple magnification devices such as the magnifying glass, loupes, and eyepieces for telescopes and microscopes.

Compound microscope

A compound microscope uses a lens close to the object being viewed to collect light (called the objective lens) which focuses an image of the object inside the microscope (image 1). That image is then magnified by a second lens or group of lenses (called the eyepiece) that gives the viewer an enlarged inverted virtual image of the object (image 2). The use of a compound objective/eyepiece combination allows for much higher magnification. Common compound microscopes often feature exchangeable objective lenses, allowing the user to quickly adjust the magnification. A compound microscope also enables more advanced illumination setups, such as phase contrast.

Other microscope variants

There are many variants of the compound optical microscope design for specialized purposes. Some of these are physical design differences allowing specialization for certain purposes:

- Stereo microscope, a low-powered microscope which provides a stereoscopic view of the sample, commonly used for dissection.
- Comparison microscope, which has two separate light paths allowing direct comparison of two samples via one image in each eye.
- Inverted microscope, for studying samples from below; useful for cell cultures in liquid, or for metallography.
- Fiber optic connector inspection microscope, designed for connector end-face inspection
- Traveling microscope, for studying samples of high optical resolution.

Other microscope variants are designed for different illumination techniques:

- Petrographic microscope, whose design usually includes a polarizing filter, rotating stage and gypsum plate to facilitate the study of minerals or other crystalline materials whose optical properties can vary with orientation.
- Polarizing microscope, similar to the petrographic microscope.
- Phase contrast microscope, which applies the phase contrast illumination method.
- Epifluorescence microscope, designed for analysis of samples which include fluorophores.
- Confocal microscope, a widely used variant of epifluorescent illumination which uses a scanning laser to illuminate a sample for fluorescence.
- Two-photon microscope, used to image fluorescence deeper in scattering media and reduce photobleaching, especially in living samples.
- Student microscope – an often low-power microscope with simplified controls and sometimes low quality optics designed for school use or as a starter instrument for children.[6]
- Ultra microscope, an adapted light microscope that uses scattering to allow viewing of tiny particles whose diameter is below or near the wavelength of visible light (around 500 nanometers); mostly obsolete since the advent of electron microscopes

Digital microscope

A digital microscope is a microscope equipped with a camera allowing observation of a sample via a computer. Microscopes can also be partly or wholly computer-controlled with various levels of automation. Digital microscopy allows greater analysis of a microscope image, for example measurements of distances and areas and quantitation of a fluorescent or histological stain.

Low-powered digital microscopes, USB microscopes, are also commercially available. These are essentially webcams with a high-powered lens and generally do not use Trans illumination. The camera attached directly to the USB port of a computer, so that the images are shown directly on the monitor. They offer modest magnifications (up to about 200×) without the need to use eyepieces, and at very low cost. High power illumination is usually provided by an LED source or sources adjacent to the camera lens.

Digital microscopy with very low light levels to avoid damage to vulnerable biological samples is available using sensitive photon-counting digital cameras. It has been demonstrated that a light source providing pairs of entangled photons may minimize the risk of damage to the most light-sensitive samples. In this application of ghost imaging to photon-sparse microscopy, the sample is illuminated with infrared photons, each of which is spatially correlated with an entangled partner in the visible band for efficient imaging by a photon-counting camera

Lighting techniques

While basic microscope technology and optics have been available for over 400 years it is much more recently that techniques in sample illumination were developed to generate the high quality images seen today.

In August 1893 August Koehler developed Koehler illumination. This method of sample illumination gives rise to extremely even lighting and overcomes many limitations of older techniques of sample illumination. Before development of Koehler illumination the image of the light source, for example a light bulb filament, was always visible in the image of the sample.

The Nobel Prize in physics was awarded to Dutch physicist Frits Zernike in 1953 for his development of phase contrast illumination which allows imaging of transparent samples. By using interference rather than absorption of light, extremely transparent samples, such as live mammalian cells, can be imaged without having to use staining techniques. Just two years later, in 1955, Georges Nomarski published the theory for differential interference contrast microscopy, another interference-based imaging technique

Fluorescence microscopy

Modern biological microscopy depends heavily on the development of fluorescent probes for specific structures within a cell. In contrast to normal Trans illuminated light microscopy, in fluorescence microscopy the sample is illuminated through the objective lens with a narrow set of wavelengths of light. This light interacts with fluorophores in the sample which then emit light of a longer wavelength. It is this emitted light which makes up the image.

Since the mid-20th century chemical fluorescent stains, such as DAPI which binds to DNA, have been used to label specific structures within the cell. More recent developments include immunofluorescence, which uses fluorescently labelled antibodies to recognize specific proteins within a sample, and fluorescent proteins like GFP which a live cell can express making it fluorescent.

Components:

All modern optical microscopes designed for viewing samples by transmitted light share the same basic components of the light path. In addition, the vast majority of microscopes have the same 'structural' components [28] (numbered below according to the image on the right):

- Eyepiece (ocular lens) (1)
- Objective turret, revolver, or revolving nose piece (to hold multiple objective lenses) (2)
- Objective lenses(3)
- Focus knobs (to move the stage)
    - Coarse adjustment (4)
    - Fine adjustment (5)
- Stage (to hold the specimen) (6)
- Light source (a light or a mirror) (7)
- Diaphragm and condenser (8)
- Mechanical stage (9)

Eyepiece (ocular lens)

The eyepiece, or ocular lens, is a cylinder containing two or more lenses; its function is to bring the image into focus for the eye. The eyepiece is inserted into the top end of the body tube. Eyepieces are interchangeable and many different eyepieces can be inserted with different degrees of magnification. Typical magnification values for eyepieces include 5×, 10× (the most common), 15× and 20×. In some high performance microscopes, the optical configuration of the objective lens and eyepiece are matched to give the best possible optical performance. This occurs most commonly with apochromatic objectives.

Objective turret (revolver or revolving nose piece)

Objective turret, revolver, or revolving nose piece is the part that holds the set of objective lenses. It allows the user to switch between objective lenses.

Objective

At the lower end of a typical compound optical microscope, there are one or more objective lenses that collect light from the sample. The objective is usually in a cylinder housing containing a glass single or multi-element compound lens. Typically there will be around three objective lenses screwed into a circular nose piece which may be rotated to select the required objective lens. These arrangements are designed to be par focal, which means that when one changes from one lens to another on a microscope, the sample stays in focus. Microscope objectives are characterized by two parameters, namely, magnification and numerical aperture. The former typically ranges from 5× to 100× while the latter ranges from 0.14 to 0.7, corresponding to focal lengths of about 40 to 2 mm, respectively. Objective lenses with higher magnifications normally have a higher numerical aperture and a shorter depth of field in the resulting image. Some high performance objective lenses may require matched eyepieces to deliver the best optical performance

Oil immersion objective

Some microscopes make use of objectives or water-immersion objectives for greater resolution at high magnification. These are used with material such as immersion oil or water and a matched cover slip between the objective lens and the sample. The refractive index of the index-matching material is higher than air allowing the objective lens to have a larger numerical aperture (greater than 1) so that the light is transmitted from the specimen to the outer face of the objective lens with minimal refraction. Numerical apertures as high as 1.6 can be achieved. The larger numerical aperture allows collection of more light making detailed observation of smaller details possible. An oil immersion lens usually has a magnification of 40 to 100×

Focus knobs

Adjustment knobs move the stage up and down with separate adjustment for coarse and fine focusing. The same controls enable the microscope to adjust to specimens of different thickness. In older designs of microscopes, the focus adjustment wheels move the microscope tube up or down relative to the stand and had a fixed stage.

Frame

The whole of the optical assembly is traditionally attached to a rigid arm, which in turn is attached to a robust U-shaped foot to provide the necessary rigidity. The arm angle may be adjustable to allow the viewing angle to be adjusted.

The frame provides a mounting point for various microscope controls. Normally this will include controls for focusing, typically a large knurled wheel to adjust coarse focus, together with a smaller knurled wheel to control fine focus. Other features may be lamp controls and/or controls for adjusting the condenser.

Stage

The stage is a platform below the objective which supports the specimen being viewed. In the center of the stage is a hole through which light passes to illuminate the specimen. The stage usually has arms to hold slides (rectangular glass plates with typical dimensions of 25×75 mm, on which the specimen is mounted).

At magnifications higher than 100× moving a slide by hand is not practical. A mechanical stage, typical of medium and higher priced microscopes, allows tiny movements of the slide via control knobs that reposition the sample/slide as desired. If a microscope did not originally have a mechanical stage it may be possible to add one.

All stages move up and down for focus. With a mechanical stage slides move on two horizontal axes for positioning the specimen to examine specimen details.

Focusing starts at lower magnification in order to center the specimen by the user on the stage. Moving to a higher magnification requires the stage to be moved higher vertically for re-focus at the higher magnification and may also require slight horizontal specimen position adjustment. Horizontal specimen position adjustments are the reason for having a mechanical stage.

Due to the difficulty in preparing specimens and mounting them on slides, for children it's best to begin with prepared slides that are centered and focus easily regardless of the focus level used.

Light source

Many sources of light can be used. At its simplest, daylight is directed via a mirror. Most microscopes, however, have their own adjustable and controllable light source – often a halogen lamp, although illumination using LEDs and lasers are becoming a more common provision. Koehler illumination is often provided on more expensive instruments.

Condenser

The condenser is a lens designed to focus light from the illumination source onto the sample. The condenser may also include other features, such as a diaphragm and/or filters, to manage the quality and intensity of the illumination. For illumination techniques like dark field, phase contrast and differential interference contrast microscopy additional optical components must be precisely aligned in the light path.

Magnification

The actual power or magnification of a compound optical microscope is the product of the powers of the ocular (eyepiece) and the objective lens. The maximum normal magnifications of the ocular and objective are 10× and 100× respectively, giving a final magnification of 1,000.

Magnification and micrographs

When using a camera to capture a micrograph the effective magnification of the image must take into account the size of the image. This is independent of whether it is on a print from a film negative or displayed digitally on a computer screen.

In the case of photographic film cameras the calculation is simple; the final magnification is the product of: the objective lens magnification, the camera optics magnification and the enlargement factor of the film print relative to the negative. A typical value of the enlargement factor is around 5× (for the case of 35 mm film and a 15 × 10 cm (6 × 4 inch) print).

In the case of digital cameras the size of the pixels in the CMOS or CCDdetector and the size of the pixels on the screen have to be known. The enlargement factor from the detector to the pixels on screen can then be calculated. As with a film camera the final magnification is the product of: the objective lens magnification, the camera optics magnification and the enlargement factor.

Other techniques

Modern microscopes allow more than just observation of transmitted light image of a sample; there are many techniques which can be used to extract other kinds of data. Most of these require additional equipment in addition to a basic compound microscope.

- Reflected light, or incident, illumination (for analysis of surface structures)
- Fluorescence microscopy, both:
    - Epifluorescence microscopy
    - Confocal microscopy
- Micro spectroscopy (where a UV-visible spectrophotometer is integrated with an optical microscope)
- Ultraviolet microscopy
- Near-Infrared microscopy
- Multiple transmission microscopy for contrast enhancement and aberration reduction.
- Automation (for automatic scanning of a large sample or image capture)

Applications

Optical microscopy is used extensively in microelectronics, nanophysics, biotechnology, pharmaceutics research, mineralogy and microbiology.

Optical microscopy is used for medical diagnosis, the field being termed histopathology when dealing with tissues, or in smear tests on free cells or tissue fragments.

In industrial use, binocular microscopes are common. Aside from applications needing true depth perception, the use of dual eyepieces reduces strain associated with long workdays at a microscopy station. In certain applications, long-working-distance or long-focus microscopes are beneficial. An item may need to be examined behind a window, or industrial subjects may be a hazard to the objective. Such optics resemble telescopes with close-focus capabilities

Measuring microscopes are used for precision measurement. There are two basic types. One has a reticle graduated to allow measuring distances in the focal plane. The other (and older) type has simple crosshairs and a micrometer mechanism for moving the subject relative to the microscope.

KARPAGAM ACADEMY OF HIGHER EDUCATION, COIMBATORE-21
DEPARTMENT OF PHYSICS
CLASS : I M.SC PHYSICS
BATCH: 2018-2020
PART A : MULTIPLE CHOICE QUESTIONS (ONLINE EXAMINATIONS)
SUBJECT : MATERIAL CHARACTERIZATION
SUBJECT CODE : 18PHP105A
UNIT-III

SL.NO.	QUESTIONS	opt 1	opt2	opt3	opt4	Answer
1	In the crystal growth process,supersaturation will be attained ……	when temperature increases	when temperature decreases	when salt dissolves completely	none of these	when temperature increases
2	Heterogeneous nucleation is typically much faster than homogeneous nucleation because nucleation barrier is ……..at a surface	higher	much lower	much higher	lower	much lower
3	The solubility diagram is between temperature and ……	concentration	time	pressure	none of these	concentration
4	Bridgman crystal growth method is based on ………	gel growth	solution growth	melt growth	vapour growth	melt growth
5	The spontaneous formation of crystalline nuclei in the interior of the parent phase is called …..	Homogeneous nucleation	heterogeneous nucleation	instability	seed	Homogeneous nucleation
6	A crucible used in the bridgman crystal growth method is………….	quartz	glass	plastics	metals	quartz
7	The gibbs free energy changes from ………	0 to infinity	-1 to 0	0 to 1	none of these	0 to infinity
8	The solubility of most substances …………….. With temperature	does not relate	increases	decreases	none of these	increases
9	According to BCF theory, the important factor for growth parameter is……..	surface diffusion	volume diffusion	ternary growth	pressure	surface diffusion
10	The vapour transport is carried out in ………	crucibles	Al rod	quartz	silicon	Al rod
11	An example for physical gel is ………	silica	polyacrylamide	tetramethoxy silane	agar-agar	silica
12	A decrease of crystal ………………is demanded simultaneously with the development of greater crystal dimensions	defects	quality	inhomogeneities	both a and c	both a and c
13	The photonic device evolution is due to the advent of ………………….. Crystals	compound semiconductor	metal-organic	organic	inorganic	compound semiconductor
14	The major use of GaAs at present is in the area of ……..	microwave devices	high speed digital integrated circuits	substrates for epitaxial layer growth	all the above	all the above
15	InP is well established as the base material for …….	optical components	electronic component	mechanical component	opto-electronic components	opto-electronic components
16	The ………………… are among the most widespread type of scintillation materials	oxide crystals	organic crystals	halogenide scintillators	quartz	halogenide scintillators
17	Alkali halide scintillators like ……..	NaI:TI	KMgF3	CsCaBr3	RbMgF3	NaI:TI
18	Fluorperovskites such as ……..	CsSrBr3	LiF:Eu	CsI	LiF:Eu	CsSrBr3
19	The applications of alkali halide scintillators are ……..	UV applications	ultrasound applications	IR optics	all the above	all the above
20	Pick one of the requirements for the scintillators……..	slow scintillation decay	fast scintillation rise	low light yield	slow scintillation rise	fast scintillation rise
21	Attractive oxide scintillation crystals are …….	BGO	KCaF3	NaI:TI	KDP	BGO
22	Nonlinear optical crystals are very important for…...	Jewelry	watch	scintillation	laser frequency conversion	laser frequency conversion
23	KDP is a suitable crystal for ………….. Of huge laser systems for fusion experiments	high harmonic generation	low harmonic generation	Acousto optic crystals	semiconductors	high harmonic generation
24	KTP is …..	hygroscopic	non hygroscopic	mechanically hard	both b and c	both b and c
25	Borate crystals are used in ……..	IR optics	NLO	coherent UV sources	all the above	coherent UV sources
26	The success of the borate crystals can be attributed to the unique structural characteristics of …………. Groups	boron-oxygen	boron	oxygen	halide	boron-oxygen
27	Pick one of the following which is promising for UV generation	beta-barium borate	LiF:Eu	KDP	KTP	beta-barium borate
28	……………. is more suitable for 4HG and 5HG of Nd:YAG laser	yittrium calcium borate	cesium lithium borate	KDP	KTP	cesium lithium borate
29	………….. are suitable for 2nd and 3rd harmonic generation of Nd:YAG laser radiation	YCa4O(BO3)3	GdxY1-xCa4O(BO3)3	cesium lithium borate	both a and b	both a and b
30	Choose organic NLO materials from the following	L-Arginine phophate	urea	4-dimethylamino-N-methyl-4-stilbazolium tosylate	all the above	all the above
31	………..crystals due to the piezoelectric property and ability to rotate a plane of polarization and high transparency are used in electronics and optical instrumentation	Quartz	KDP	urea	all the above	Quartz
32	KTP is a useful nonlinear optical crystal to get efficient green light by the frequency doubling of …………….	Nd:YAG laser	He-Ne laser	Ti:Sapphire laser	all the above	Nd:YAG
33	Crystal growth is a ……………..process	non-equilibrium	equilibrium	stable	none of these	non-equilibrium
34	Many ……………. Properties of ………….. Are obscured by the effects of grain boundaries	physical and liquids	magnetic and solid	physical and solids	physical and gas	physical and solids

35	Growth methods are classified into ………..types	three	two	four	none of these	three
36	The third step in the growth of crystals is ……….	successive growth of crystals to yield distinct faces	achievement of supersaturation	formation of crystal nuclei	supercooling	successive growth of crystals to yield distinct faces
37	The cluster consisting of few atoms or molecules is called……….	nuclei	seed	crystal	polycrystal	nuclei
38	The kinetics of phase change take place in …….. Different stages	five	three	four	two	four
39	The development of the supersaturated state may arise due to change in……….	temperature	pressure	chemical or physical condition	all the above	all the above
40	Once embryos achieve the ………. Size there is a high probability that they will grow	nano	micro	bulk	critical	critical
41	critical nuclei have more …….. than bulk phases of the same mass	pressure	concentration	energy	energy and concentration	energy
42	William Thomson showed that the vapour pressure of a liquid in the form of a drop o radius r is greater than	vapour pressure over a plane liquid surface	saturation vapour pressure over a plane liquid surface	vapour pressure inside a liquid	none of these	saturation vapour pressure over a plane liquid surface
43	J.J.Thomson modified Thomsons equation to show that the melting point of a small crystal is …….of a crystal	less than that	more than that	equal	a or b	less than that
44	Since the two phases(i.e. crystal and supercooled melt) are in equilibrium, their chemical potentials must be	equal	not equal	high	low	equal
45	The solubility of a crystal increases as the size of the crystal…………….	decreases	increases	not changes	a or b	decreases
46	If C_1 and C_∞ are the concentrations of solution with a small crystal of radius r and wit a large crystal of radius r =∞ respectively then	$KTln(C_1/Ci_\infty)=2\sigma V_{II}/r$	$KTln(CI\infty/C1)=2\sigma V_{II}/r$	$KTln(C_1/CI_\infty)=2\sigma V_{II}$	$KTln(C_1/CI_\infty)=\sigma V_{II}$	$KTln(C_1/Ci_\infty)=2\sigma V_{II}/r$
47	Any crystal smaller than r will dissolve in the supersaturated solution since its solubility is …………… than C_1	lower	greater	equal	a or b	greater
48	The size corresponding to the maximum free change is called ………	nucleus	small nucleus	critical nucleus	large nucleus	critical nucleus
49	The surface energy term……… with r^2 and the volume energy term …….. With r^3	decreases, increases	increases,decreases	constant, increases	decreases,constant	increases,decreases
50	The free energy change associated with the critical nucleus is ……...	$\Delta G^*=16\pi\sigma^3/3\Delta G_v^2$	$\Delta G^*=16\pi\sigma^2/3\Delta G_v^2$	$\Delta G^*=\pi\sigma^3/3\Delta G_v^2$	$\Delta G^*=16\pi\sigma^3/\Delta G_v^2$	$\Delta G^*=16\pi\sigma^3/3\Delta G_v^2$
51	The expression for ΔG_v for the nucleation from solution is given by…………	$\Delta G_v=-(kT/v)lnS$	$\Delta G_v=(kT/v)lnS$	$\Delta G_v=-(kT)lnS$	$\Delta G_v=-lnS$	$\Delta G_v=-(kT/v)lnS$
52	The number of critical nuclei formed per unit time per unit volume is known as the ……..	rate of formation	nucleation	rate of nucleation	seed growth	rate of nucleation
53	The nucleation on the surface of a nucleant is known as……….	heterogeneous nucleation	homogeneous nucleation	homo or heterogeneous nucleation	none of these	heterogeneous nucleation
54	The concentration of the critical nuclei is given as ……..	$C(i^*)=C(1)exp[-\Delta G(i^*)]$	$C(i)=C(1)exp[\Delta G(i^*)/kT]$	$C(i^*)=exp[\Delta G(i^*)/kT]$	$C(i^*)=C(1)exp[-\Delta G(i^*)/kT]$	$C(i^*)=C(1)exp[-\Delta G(i^*)/kT]$
55	σ_{sv} is the interfacial energies between ……..	liquid-substrate	vapour-substrate	vapour-solid	substrate-vapour	vapour-substrate
56	The frequency of the continuous X-rays emitted from the tube……	do not depend on the target	depends only on the potential difference	directly proportional to the potential difference	all of the above	all of the above
57	The frequencies of the characteristic X-rays emitted from an X-ray tube	do not depend on potential difference	depends only on the atomic number of the target	can be increased by increasing atomic number of target	all of the above	all of the above
58	The penetrating power of X-rays emitted from an X-ray tube depends on	filament current	applied potential difference	atomic number of target	both b and c	both b and c
59	which of the following can be deflected by an electric field	X-rays	UV-rays	cathode rays	microwaves	cathode rays
60	The order of the wavelength of X-rays is	10^{-10}m	1m	10^{-6}m	10^{-4}Å	10^{-10}m

SYLLABUS

Electron Microscopy

Electron diffraction technique – High energy electron diffraction – Low energy electron diffraction - Electron microscopy – Scanning electron microscopy (SEM) - FESEM - EDAX - TEM - HRTEM: working principle and Instrumentation - sample preparation - Advantages/disadvantages.

Scanning Probe Microscopy

Scanning probe microscopy - STM - AFM - EPMA - working principle and Instrumentation - Advantages/disadvantages.

LOW-ENERGY ELECTRON DIFFRACTION

Low-energy electron diffraction (LEED) is a powerful method for determining the geometric structure of solid surfaces. The phenomenon was first observed by Davisson and Germer in 1927 and provided the earliest direct experimental proof of the wavelike properties of electrons. LEED has since evolved into one of the most powerful and widespread tools of the surface scientist. It is similar to xray diffraction (XRD) in the type of information that it provides, and XRD will be frequently referred to for analogy throughout this unit. The most obvious difference is that a beam of electrons, rather than x rays, is used. Since electrons have a mean free path (or attenuation length) measured in angstroms (A°) as opposed to microns (m) for x rays, LEED is particularly sensitive to surface geometry.

LEED is a structural technique that can provide essentially two levels of information. In both cases, it is most commonly used to determine the structure of a solid surface when the bulk structure of the material is already known by other means (e.g., XRD). It is possible, and indeed straightforwardly simple, to use LEED to determine both the absolute dimensions of the surface unit cell and the unit cell symmetry. One can easily deduce that, for example, a surface has a two-dimensional (2D) unit cell twice as large as that of the bulk; this often allows a reasonable guess at the true structure. Sometimes it is sufficient to know that a particular phase is present without knowing the details of the structure.

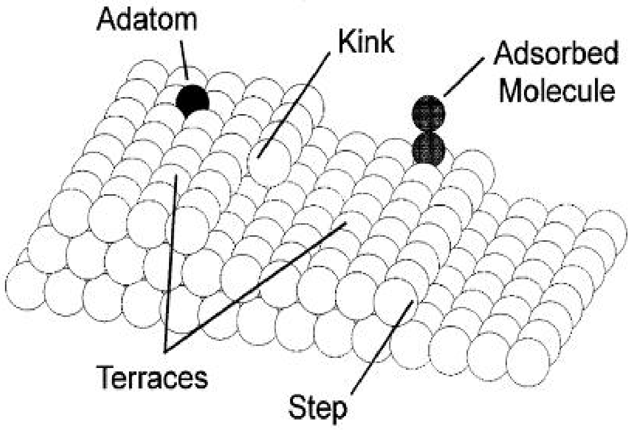

For example, the (2 _ 4) reconstruction of GaAs (nomenclature explained below) has been found to be optimal for device growth Farrow, 1995). Determination of the exact atomic positions is more difficult, but quantitative experiments can elucidate this second level of information. Sophisticated calculations, generally run on a workstation, can provide atomic coordinates with a typical precision of _0.05 A which is generally more than adequate to determine the adsorption site of a molecule or the atomic positions in a reconstructed surface.

Many different surfaces can be examined by LEED, and their terminology must be understood. We assume familiarity with the basic crystal structures [face-centered cubic (fcc), zincblende, etc.]. A particular crystal face is specified by its Miller indices. These are of the form (hkl), and the ideal bulk termination can be determined in the following way: place one corner of the unit cell at the origin of a Cartesian coordinate system and construct a plane that intersects the axes at the reciprocal of the respective Miller index (see SYMMETRY IN CRYSTALLOGRAPHY). In the general case, this plane would pass through the points (1/h, 0, 0), (0, 1/k, 0), and (0, 0, 1/l). A Miller index of zero indicates that the plane is parallel to that axis. Further examples can be found in any solid-state textbook (e.g., Ashcroft and Mermin, 1976; Kittel, 1986). It is conceptually useful to regard a surface as being composed of stacked planes of atoms, each parallel to the topmost surface plane (see SYMMETRY IN CRYSTALLOGRAPHY).

The structure of an actual surface is usually very different from an ideal termination of the bulk. The low-Miller- index surfaces—(100), (110), (111)—are relatively flat, but higher-index surfaces generally have a large number of steps and often kinks as well. Adatoms and adsorbed molecules also appear in many systems. Figure 1 illustrates some of these features. LEED is sensitive to any such structures that recur at regular intervals, that is, with measurable periodicity. LEED is a mature area of surface science and it is useful to consider the state of the art in this field. A great deal of work has been done on clean metal and semiconductor surfaces, and much of this is considered ‘‘done’’; current work in this area consists mostly of refinements. Most low-index clean metal surfaces are found to merely relax the spacing between the topmost layers. Higher-index metal surfaces tend to be less closely packed and more prone to reconstruction. Clean semiconductor surfaces almost always reconstruct. Adsorbed atoms and molecules are sometimes found to lift reconstructions, and they often modify the dimensions and orientation of the surface unit cell themselves. Several atoms and simple molecules (H, O, S, CO, C2H) have been investigated on low-Miller-indexsurfaces of semiconductors (Si, GaAs) and most transition metals. An important direction of current research is the growth of ordered crystalline epitaxial films for a variety of purposes. They serve as models for catalytic systems (Boffa et al., 1995), model magnetic structures, or avenues for studying otherwise intractable systems (Roberts et al; 1998), to name a few examples. Other recent advances seek to extend the power of the technique to systems 4 with disorder in geometry (Do¨l et al., 1997; Starke et al.,1996) or composition authier et al., 1985; Crampin et al.,1991). Because of the time-consuming trial-and-error computations involved in a structural determination, there is also interest in developing a LEED-ased holographic technique for rapid adsorption site determination (Saldin,1997).

SCANNING ELECTRON MICROSCOPY (SEM)

In scanning electron microscope, electron beam scans across the sample surface and collects scattered electrons for imaging. Because the image is formed using backscattered signals instead of forward-transmitted signals, the electron beam energy does not need to be high (~40 keV) and the sample also does not require electronic transparency; it has only a conductivity requirement to prevent charging.

Scanning electron microscopy (SEM) is one of the most widely used techniques for the characterization. SEM is providing not only topographical information like optical microscopes but also information of chemical composition near the surface. SEM creates magnified images by using electrons instead of light. It gives detailed 3-D images at higher magnification than an optical microscope. The various processes of interaction of primary electron beam with specimen in an electron microscope are shown in Figure 2.7. In the scanning electron microscope, back scattered electrons and secondary electrons are captured by a detector to form the image.

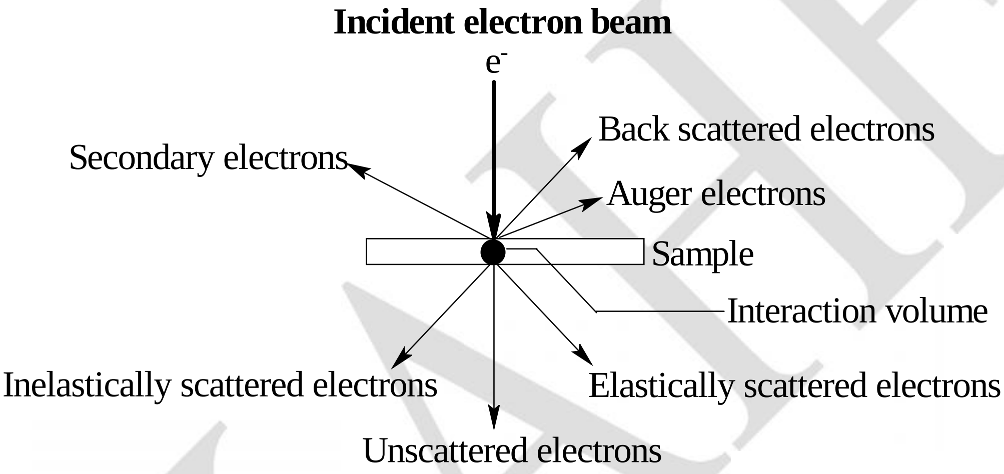

Interaction between primary electron beam and the sample in an electron microscope

Secondary electrons arise due to inelastic collision between primary electrons (the beam) and loosely bound electrons of the conduction band or tightly bound valence electrons. The energy transferred is sufficient to overcome the work function which binds them to the solid and hence they are ejected. The ejected electrons have 5-10 eV energy and they are detected by scintillator / photomultiplier tube. Back scattered electrons arise due to elastic collisions between the incoming electron and the nucleus of the target atom (i.e. Rutherford scattering). Higher the atomic number, higher is the number of back scattered electrons. They are detected by semiconductor detectors.

Most of the samples used in the study are low conducting specimens and hence the samples were coated with gold by sputtering method. The morphology of the materials were recorded using a scanning electron microscope (HITACHI COM-S-4200) operated at an accelerating voltage of 16 kV. The samples were suspended in methanol and the specimen stub was dipped into the liquid and removed. The sample powder deposited onto the surface of the stub evenly when methanol was evaporated. This specimen was coated with gold for two minutes. The beam is scanned over the specimen surface in synchronism with the beam of a cathode ray tube (CRT) display screen. Materials can be studied properly only when they are electrically conducting, otherwise they give rise to charging phenomena resulting blurred images.

Energy Dispersive X-ray Spectroscopy

Energy dispersive X-ray (EDX**)** spectroscopy is an analytical technique used for the elemental analysis of the sample. A high energy beam of electrons is focused on the sample. The incident beam of electrons excites an electron in the inner shell of an atom thus creating an electron-hole. An electron from an outer higher energy shell then fills the hole. The difference in energy between higher energy and lower energy shell may be released in the form of an X-ray. The number and energy of X-rays emitted from a specimen can be measured by an energy dispersive spectrometer. As the energy of X-rays is characteristic of the difference in energy between the two shells and atomic structure of the element from which they are emitted, this allows the elemental identification and hence the composition of the specimen to be measured. The detector converts X-ray energy into voltage signals and the information is sent to the pulse processor, which measures the signals and passes them onto an analyzer for data display and analysis.

A silicon semiconductor is used with high impedance zone which is radiation sensitive. Each absorbed X-ray quantum is converted into a cloud which consists of pairs of charge carriers i.e. electrons and holes. Hence, the energy of the X-ray photons can be calculated. Due to high voltage, which is applied between both ends of the sensitive area of the detector, the charge carriers are moved and collected at the ends of the sensitive zone. With a charge sensitive preamplifier, the charge quantity is finally converted into a voltage pulse. The pulse is amplified and shaped in a spectroscopic amplifier.

TRANSMISSION ELECTRON MICROSCOPY (TEM)

Transmission Electron Microscopy (TEM) has, in three decades time, become a mainstay in the repertoire of characterization techniques for materials scientists. TEM's strong cards are its high lateral spatial resolution (better than 0.2 nrn "point-to-point'' on some instruments) and its capability to provide both image and diffraction information from a single sample. In addition, the highly energetic beam of electrons used in TEM interacts with sample matter to produce characteristic radiation and particles; these signals often are measured to provide materials characterization using EDS, EELS, **EXELFS,** backscattered and secondary electron imaging, to name a few possible techniques.

Basic Principles

In TEM, a focused electron beam is incident on a thin (less than 200 nm) samplr. The signal in TEM is obtained from both undeflected and deflected electrons that penetrate the sample thickness. **A** series of magnetic lenses at and below the sample position are responsible for delivering the signal to a detector, usually a fluorescent screen, a film plate, **or** a video camera. Accompanying this signal transmission is a magnification of the spatial information in the signal by as little as 50 times to as much as a factor of 10'. This remarkable magnification range is facilitated by the small wavelength of the incident electrons, and is the key to the unique capabilities associated with TEM analysis. A schematic of a TEM instrument, showing the location of a thin sample and the principal lenses within a TEM column, is illustrated in Figure 1a.Figure Ib shows a schematic for the ray paths of both unscattered and scattered electrons beneath the sample.

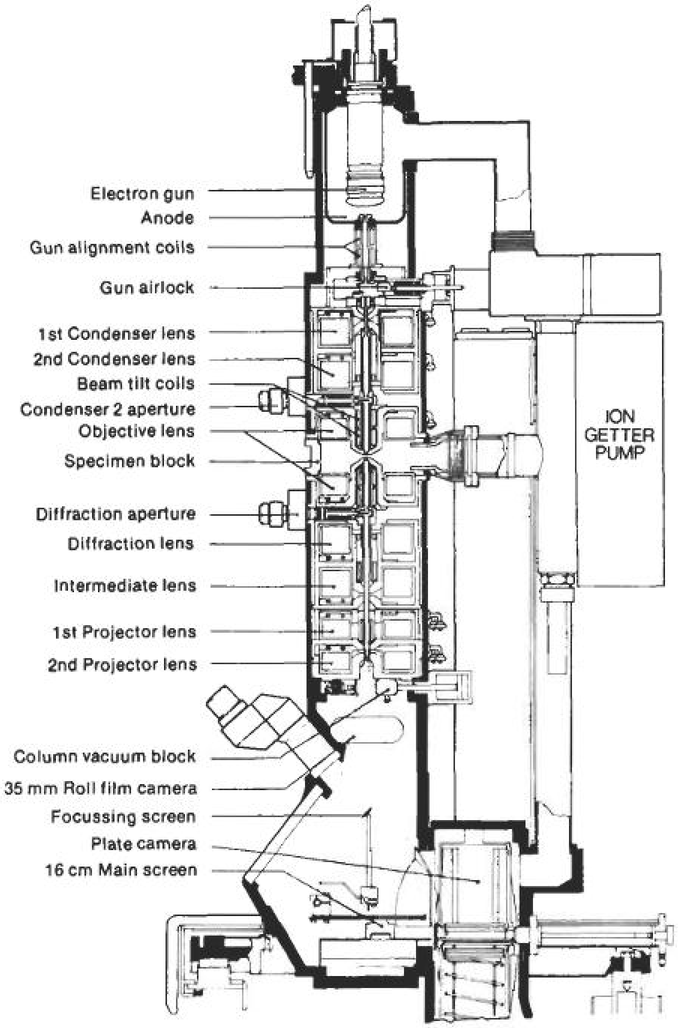

Schematic diagram a TEM instrument

Resolution

The high lateral spatial resolution in a TEM instrument is a consequence of several features of the technique. First, in the crudest sense, TEM has high spatial resolution because it uses a highly focused electron beam **as** a probe. This probe is focused at the specimen to a small spot, often ap or less in diameter. More importantly, the probe's source is an electron gun designed to emit a highly coherent beam of monoenergetic electrons of exceedingly small wavelength. The wavelength, **h,** of **IO0** keV electrons is only 0.0037 nm, much smaller than that of light, X rays, or neutrons used in other analytical techniques. Having such small wavelengths, since electrons in a TEM probe are in phase **as** they enter the specimen, their phase relationships upon exiting are correlated with spatial associations between scattering centers (atoms) within the material. Finally, high lateral spatial resolution is maintained via the use of extremely thin samples. In most TEM experiments, samples are thinned usually to less than 200 nm. For most materials this insures relatively **few** scattering events as each electron traverses the sample. Not only does this limit spreading of the probe, but much of the coherency of the incident source is **also** retained.

ATOMIC FORCE MICROSCOPY (AFM)

The ability of AFM to create three-dimensional micrographs with resolution down to nanometer scale renders it as an essential tool for imaging the surfaces. It provides nanoscale to atomic-scale microscopy by measuring the tip-surface interactions from forces and translating these to a sensor to provide information on the topographic features of the surface. The forces involved include van der Waals, electrostatic, frictional and magnetic. Typically, forces measured are in the range 10^{-3} to 10^{-6} N. The small probe-sample separation makes it possible to take measurements over a small area. AFM operates by measuring attractive or repulsive forces between a tip and the sample.

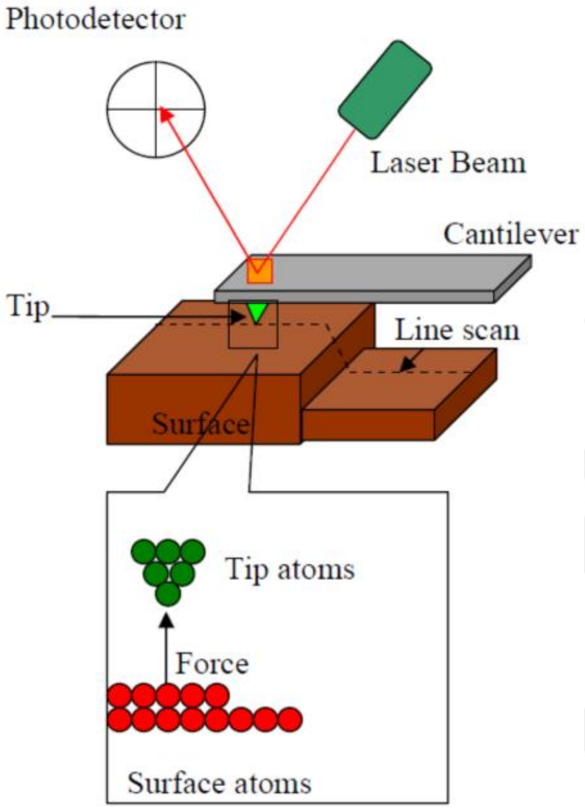

Schematic diagram of Atomic Force Microscope (AFM)

In a typical instrument (Figure 2.8), an atomically sharp tip is made to scan over a surface with feedback mechanisms that enable the piezoelectric scanners to maintain the tip at a constant force (to obtain height information), or height (to obtain force information) above the sample surface. Tips are typically made from Si_3N_4 or Si, and extended down from the end of a cantilever. The nanoscope AFM head employs an optical detection system in which the tip is attached to the underside of a reflective cantilever. A diode laser is focused onto the back of a reflective cantilever. As the tip scans the surface of the sample, moving up and down with the contour of the surface, the laser beam is deflected off the attached cantilever into a dual element photodiode. The photodetector measures the difference in light intensities between the upper and lower photodetectors, and then converts to voltage. Feedback from the photodiode difference signal, through software control from the computer, enables the tip to maintain either a constant force or constant height above the sample. In the constant force mode the piezoelectric transducer monitors real time height deviation. In the constant height mode the deflection force on the sample is recorded. The latter mode of operation requires calibration parameters of the scanning tip to be inserted in the sensitivity of the AFM head during force calibration of the microscope. The primary purpose of this instrument is to quantitatively measure surface roughness with a nominal 5 nm lateral and 0.01 nm vertical resolutions on all types of samples. Three dimensional topographical maps of the surface are then constructed by plotting the local sample height versus horizontal probe tip position. Image contrast can be achieved in many ways. The three main classes of interactions are contact mode, tapping mode and non-contact mode.

Contact mode is the most common method of operation of the AFM. As the name suggests, the tip and sample remain in close contact as the scanning proceeds. As the tip is moved for raster-scan across the surface, it gets deflected as it moves over the surface corrugation. In constant force mode, the tip is constantly adjusted to maintain a constant deflection, and therefore constant height above the surface. It is this adjustment that is displaced as data. However, the ability to track the surface in this manner is limited by the feedback circuit. Sometimes the tip is allowed to scan without this adjustment, and one measures only the deflection. This is useful for small, high speed atomic resolution scans, and is known as variable-deflection mode. Because the tip is in hard contact with the surface, the stiffness of the lever needs to be less that the effective spring constant holding atoms together, which is in the order of 1–10 nN / nm. Most contact mode levers have a spring constant of < 1 N/m.

Tapping mode is also frequently used in AFM. When operated in air or other gases, the cantilever is oscillated at its resonant frequency (often hundreds of kilohertz) and positioned above the surface so that it only taps the surface for a very small fraction of its oscillation period. This is still contact with the sample, but the very short time over which this contact occurs means that lateral forces are dramatically reduced as the tip scans over the surface. When imaging poorly immobilized or soft samples, tapping mode may be a far better choice than contact mode for imaging. The advantage of tapping the surface is improved lateral resolution on soft samples. In a non-contact mode, a stiff cantilever is oscillated in the attractive regime, meaning that the tip is quite close to the sample, but not touching it. The forces between the tip and sample are quite low, on the order of pico Newton (10^{-12} N). The detection scheme is based on measuring changes to the resonant frequency or amplitude of the cantilever. This is a very difficult mode to operate in ambient conditions with the AFM.

KARPAGAM ACADEMY OF HIGHER EDUCATION, COIMBATORE-21
DEPARTMENT OF PHYSICS
CLASS : I M.SC PHYSICS
BATCH: 2018-2020
PART A : MULTIPLE CHOICE QUESTIONS (ONLINE EXAMINATIONS)
SUBJECT : MATERIAL CHARACTERIZATION
SUBJECT CODE : 18PHP105A
UNIT-IV

SL.NO.	QUESTIONS	opt 1	opt2	opt3	opt4	Answer
1	In Bridgman technique, the rates of movement are mostly in the range………	1-30mm/hr	0.1-200mm/hr	200-300mm/hr	above 300mm/hr	1-30mm/hr
2	The advantages of the Bridgman technique are………	low-cost	suitable for low melting point materials	adhesion of the solid materials to the ampoule wall	both a and b	both a and b
3	In Bridgman technique, the melt temperature …………. With distance from the solid-liquid interface	decreases	increases	increases or decreases	constant	increases
4	A disadvantage in Bridgman technique is……..	nucleate dislocations in the material	low-cost	adhesion of the solid materials to thee ampoule wall	both a and c	both a and c
5	The container wall acts as a preferential, spurious nucleation site, resulting in……..	polycrystalline growth	single crystal growth	amorphous growth	single or polycrystal growth	polycrystalline growth
6	The requirement that the freezing isotherm should move systematically through the molten charge can be satisfied by moving	the crucible	the furnace	changing the furnace temperature	any one of the above	any one of the above
7	The Bridgman technique cannot be used for materials which……..	decompose before melting	undergo solid state phase transformation	decompose after melting	both a and b	both a and b
8	Bridgman technique is best suited for……..	high melting point materials	high vapour pressure materials	low melting point materials	both high and low melting point materials	low melting point materials
9	The characteristic of a container………	not react with the melt	smaller coefficient of thermal expansion than the crystal	smaller thermal conductivity than the crystal	all the above	all the above
10	The materials with covalently bound crystals are often compatible with containers made of …….	glasses	gold	silver	platinum	glasses
11	Graphite crucible is a useful container material for ……..	ionic materials	some covalently bound materials	some metallic materials	all the above	all the above
12	which one of the following comes under crystal pulling technique	Bridgman	zone refining	skull melting	Czochralski	Czochralski
13	Which method can produce crystals, weighing from several grams to many kilograms	crystal pulling	zone melting	slow evaporation	chemical vapour deposition	crystal pulling
14	crystal growth is a complex process, which usually takes place by a…….	phase change	solid phase	liquid phase	vapour phase	phase change
15	Irregular convective flow in crystal pulling can be produced due to……	higher temperature gradients	concentration gradients	high vapour pressure	both a and b	higher temperature gradients
16	The seed is withdrawn from the melt at such a rate that the crystal ………. Is gradually increased to its desired value	length	weight	diameter	both length and diameter	diameter
17	Growth at constant diameter is maintained by adjustments of the……	rate of pulling	rate of liquid level drop	heat fluxes into and out of the system	all the above	all the above
18	The seed can be pulled from the melt at a rate which matches the rate at which liquid crystallizes on the	seed	container	crystal	puller	seed
19	With angle of contact $\theta<0$ the crystal will……	narrow	parallel	grow out	either b or c	narrow
20	With angle of contact $\theta=0$ the crystal will……….	narrow	parallel	grow out	either a or c	parallel
21	With angle of contact $\theta>0$ the crystal will…….	parallel	narrow	grow out	either a or b	grow out
22	The terminology necking means reducing the dia gradually to grow as a…………. In diameter	2-3mm	10mm	40mm	0.5mm	2-3mm
23	The pull rod provides rotation and facility to lift and lower the crystal in……………..method	Bridgman	czochralski	zone melting	both a and b	czochralski
24	The average growth rate can be obtained by equating the mass of the ……….. that has formed	solid	liquid	liquid or solid	solid and liquid	solid
25	The important parameter governing the onset and nature of convection pattern in melts	the thermal characteristics of the material	the aspect ratio of the container	the imposed temperature gradients	all the above	all the above
26	The Prandtl number is dependent only on the……..	contained geometry	applied temperature gradient	the thermal characteristics of the liquid	the aspect ratio of the container	the aspect ratio of the container
27	In high Prandtl number systems such as oxides, strong fluid flow is largely …………	distributed throughout the bulk	confined to boundary layer regions	confined to central regions	all the above	confined to boundary layer regions
28	In low Prandtl number materials such as metals and semiconductors the streamlines are mor generally	confined to boundary layer regions	distributed throughout the bulk	confined to central regions	none of the above	distributed throughout the bulk
29	In horizontal systems the temperature gradient is characterised by the …….	Rayleigh number	Prandtl number	Grashof number	none of the above	Rayleigh number

30	In vertically driven convection systems, the relevant dimensionless number is the…..	Rayleigh number	Prandtl number	Grashof number	none of the above	Grashof number
31	The Prandtl number is defined as the ratio……	ν/κ	QI/κ	VI/κ	ν/D	ν/κ
32	Rayleigh number Ra is defined by ………	$\alpha g d^4 \Delta T_v / \nu\kappa$	$\alpha g I^4 \Delta T_H / \nu^2$	ν/κ	VI/κ	$\alpha g d^4 \Delta T_v / \nu\kappa$
33	Grashof number Gr is defined by ……..	ν/κ	$\alpha g d^4 \Delta T_v / \nu\kappa$	$\alpha g I^4 \Delta T_H / \nu^2$	ν/D	$\alpha g I^4 \Delta T_H / \nu^2$
34	As the Rayleigh(or Grashof number) increases with increase in …………, the fluid flow begins to move by convective flow	ΔT	ν	$\alpha g I^4 \Delta T_H / \nu^2$	both a and b	ΔT
35	Typical Bridgman growth ampoules have ………aspect ratio	large d/a	small d/a	large or small d/a	none of the above	large d/a
36	Forced convection flow patterns in Czochralski melts are due to various combinations of …….	crystal rotation	seed rotation	crucible rotation	seed rotation and crucible rotation	seed rotation and crucible rotation
37	The shape of the growth surface is dependent upon its ……..	crystallographic orientation	local temperature gradient	both a and b	none of the above	both a and b
38	The simplest and the best case from the point of view of good quality growth is the ……..	concave interface	convex interface	planar interface	both a and c	planar interface
39	Which model calculates, for a given instant of growth, the global heat transfer, the shape of the solid-liquid interface, natural and forced convection	Time dependent model with imposed crystal shape	Time dependent model with unknown crystal shape	Quasi-steady state model	both a and c	Quasi-steady state model
40	The………… model calculates, as functions of time	Time dependent model with imposed crystal shape	Time dependent model with unknown crystal shape	Quasi-steady state model	both a and b	both a and b
41	In ……….. Model, the variation of the tri-junction radius as a function of time is calculated	Quasi-steady state model	Time dependent model with imposed crystal shape	Time dependent model with unknown crystal shape	both a and b	Time dependent model with unknown crystal shape
42	…………….single crystals are used in the laser systems	Nd:YAG	Ti:Al_2O_3	YAP	all the above	all the above
43	The Czochralski system for the growth of oxides incorporates an induction heating system operating at…………	455kHz	455Hz	1kHz	100Hz	455kHz
44	……….. and ………., are two ferroelectric oxides	Lithium niobate and Ti:Al_2O_3	Lithium niobate and Lithium tantalate	BGO and Lithium niobate	Aluminium and iron oxide	Lithium niobate and Lithium tantalate
45	Lithium niobate and Lithium tantalate have been widely investigated due to an …………	piezoelectricity	pyroelectricity	electro-optic property	all the above	all the above
46	Equilibrium referes to a growth speed of	0mm/min	10mm/min	2mm/min	none of these	0mm/min
47	Lithium niobate and Lithium tantalate crystals are …………	biaxial crystals	uniaxial crystals	symmetric crystals	none of the above	uniaxial crystals
48	Lithium tantalate and Lithium niobate crystals are used for ………	laser systems	surface acoustic wave	magnetic bubble devices	optical components	surface acoustic wave
49	A good ratio between the crucible diameter and the crystal diameter is……..	1	2	10	3	2
50	The size of the crystal is limited by the……………..	size of the crucible	thermal gradients in the crystallization area	pull rate	both a and b	size of the crucible
51	………………..crystal has been studied extensively for acoustic wave devices	Lithium niobate	Nd:YAG	YAP	langasite	langasite
52	Isomorphic crystals have ……………	zero temperature coefficient	large electromechanical coupling factor	congruent melting point	all the above	all the above
53	Dissociable compounds can be grown by…………	CZ method	sealed tube methods	vertical pulling methods	both b and c	both b and c
54	Pick out the suitable property of encapsulant……...	melt after the compound melts	more dense than the melt of the compound	transparent	not wet the crucible	transparent
55	Boron tri oxide has proved to be one of the best encapsulants for ……………………….type melts	metals	semiconductor	insulator	both a and b	both a and b
56	The technological importance of GaAs and InP comes about because of their use in …………………..	electronic devices	photonic devices	magnetic devices	both a and b	both a and b
57	The paper published by Pfann(1952) was related to……………….. Technique	Zone melting	Zone refining	float zone	all the above	all the above
58	In zone refining, if freezing is rapid enough, k may actually………….	approach unity	less than unity	more than unity	0 to 1	approach unity
59	………………..process is used for the growth of zirconium oxide	Zone melting	Skull melting	CZ	both a abd c	Skull melting
60	……………………..is a process, which dynamically controls both the heat input and the heat extraction in a crystal growth furnace	Skull melting	Zone melting	Bridgman	Heat exchanger	Heat exchanger

SYLLABUS

Electrical and Optical Methods of Characterisation
Two probe and four probe methods - van der Pauw method - Hall probe and measurement - scattering mechanism - C-V, I-V characteristics - Schottky barrier capacitance - impurity concentration - electrochemical C-V profiling - limitations - Introduction to Photoluminescence and Electroluminescence - Applications. Dielectrics - working principle and Instrumentation - Applications.

ELECTRICAL PROPERTIES

Electrical properties such as resistivity, carrier concentration and Hall mobility were estimated from the mobility were estimated from the four probe method and Hall measurements in van der Pauw configuration at room temperature.

FOUR-POINT COLLINEAR PROBE METHOD

The most common way of measuring the resistivity of a semiconductor material is using a four-point collinear probe (Hartnagell et al 1995). This technique involves bringing four equally spaced probes in contact with a material of unknown resistance. The probe array is placed in the centre of the material, as shown in Figure 2.9.

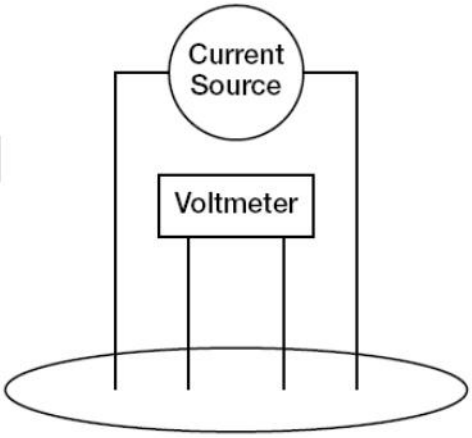

Schematic diagram of four point collinear setup

The two outer probes are used for applying the current source and the two inner probes are used for measuring the resulting voltage difference across the surface of the sample. The sheet resistance is calculated as follows,

$$R_{sh} = \frac{\circledR}{In_2} \times \frac{V}{I} \times K \qquad (2.2)$$

where, R_{sh} is the sheet resistance (Ω/cm), V is the measured voltage (volts), I is the source current (amperes), K is a correction factor based on the ratio of the probe to wafer diameter and on the ratio of wafer thickness to probe separation.

Van der Pauw configuration

The van der Pauw method involves applying a current and measuring the voltage using four small contacts on the circumference of a flat, arbitrarily shaped sample of uniform thickness (van der Pauw 1983). This method is particularly useful for measuring very small samples because geometric spacing of the contacts is unimportant. Effect due to the size of a sample, which is the approximate probe spacing, is irrelevant. Using this method, the resistivity can be derived from a total of eight measurements that are made around the periphery of the sample with the configurations shown in Figure 2.10.

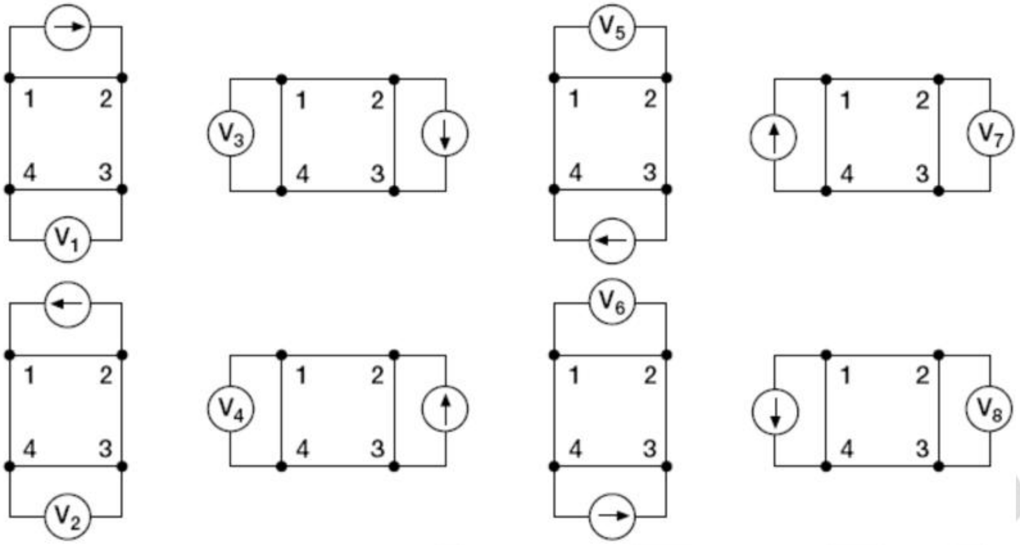

Fig. 2.10 Symmetric contacts in van der Pauw configuration

The samples used were 1 × 1 cm^2 in size and the electrical contact was established using indium metal or silver paste. The gold spring probes were placed at the corners of the sample symmetrically as shown in Figure 2.10. A constant current of 1mA was supplied to the sample. The sample was subjected to uniform magnetic field of 0.57 Tesla. A known current was passed through the electrodes of the samples and voltage across the other two electrodes was measured. The polarity was reversed for each measurement and the voltage was measured. Once all the voltage measurements are taken, two values of resistivity, ρ_A and ρ_B are derived as follows,

$$\circ_A = \frac{\circledR}{In2} f_A t_s \frac{(V_1 - V_2 + V_3 - V_4)}{4I} \qquad (2.3)$$

$$\circ_B = \frac{\circledR}{In2} f_B t_s \frac{(V_5 - V_6 + V_7 - V_8)}{4I} \qquad (2.4)$$

where, ρ_A and ρ_B are resistivities in Ω-cm, t_s is the sample thickness in nm, V_1–V_8

represents the voltages measured by the voltmeter, I is the current passed through the sample in amperes, f_A and f_B are geometrical factors based on sample symmetry. Once ρ_A and ρ_B are known, the average resistivity (ρ_{AVG}) can be determined as follows:

$$\rho_{AVG} = \frac{\rho_A + \rho_B}{2} \qquad (2.5)$$

The Hall signal is measured between two ends while the current is passing through the other two ends. Hall mobility (μ) is given by the ratio

$$\mu = \Delta R \times \frac{10^8}{BR_{sh}} \qquad (2.6)$$

where, ΔR is the change in resistance due to magnetic field (B) which was applied to measure Hall voltages and R_{sh} is sheet resistance of the material. Carrier concentration is determined using the relation

$$\rho = \frac{1}{en\mu} \qquad (2.7)$$

The Hall coefficient R_H is given by,

$$R_H = \rho \times \mu \qquad (2.8)$$

The type of carriers can be understood from the sign of the R_H and thus the type of conductivity can be identified. The negative value of R_H corresponds to the flow of electrons (n-type) and positive value corresponds to the flow of holes (p- type) (Schroder Dieter 1998).

THICKNESS MEASUREMENT

Thickness plays an important role in the properties of thin films. The results obtained can be reproduced only when the film thickness and the deposition parameters are kept constant. In the present work, the film thickness was determined by employing weight gain method, optical interference technique and stylus profilometry.

The initial estimation of thickness was done using the conventional gravimetric method. In this method, the weight of the substrates before (W_1) and after deposition (W_2) was used to find out the weight of the film deposit (W_3) by the given relation $W_3 = (W_2 – W_1)$. Thus knowing the weight of the material coated on the area and the film density (ρ_d), the thickness (t) of the film can be obtained by the relation (Elangovan and Ramamurthi 2003).

$$t = \frac{W_3}{A^{\circ}{}_d} \qquad (2.9)$$

The thickness of the layers deposited onto the glass plates was calculated from the optical interference maxima (λ_1, λ_2) appearing in the transmission spectra of the films and the refractive index (n) of the film material according to the formula (Swanepol 1983)

$$t = \frac{a_1 a_2}{2n(a_1 - a_2)} \qquad (2.10)$$

The optically and gravimetrically measured thickness was consequently verified by the stylus profilometry technique. The Hall effect measurement setup used in this work is shown in the Figure 2.11.

Hall effect measurement system used for present work

PHOTOLUMINESCENCE

Luminescence refers to the emission of light by a material through any process other than blackbody radiation. The term Photoluminescence (PL) narrows this down to any emission of light that results from optical stimulation. Photoluminescence is apparent in everyday life, for example, in the brightness of white paper or shirts (often treated with fluorescent whiteners to make them literally glow) or in the light from the coating on a fluorescent lamp. The detection and analysis **of** this emission is widely used as an analytical tool due to its sensitivity, simplicity, and low cost. Sensitivity is one of the strengths of the PL technique, allowing very small quantities (nanograms) or low concentrations (parts-per-trillion) of material to be analyzed. Precise quantitative concentration determinations are difficult unless conditions *can* be carefully controlled, and many applications of PL are primarily qualitative.

PL is often referred to **as** fluorescence spectrometry **or** fluorometry, especially when applied to molecular systems. Uses for PL are found in many fields, including environmental research, pharmaceutical and food analysis, forensics, pesticide studies, medicine, biochemistry, and semiconductors and materials research. PL can be used **as** a tool for quantification, particularly for organic materials, wherein the compound of interest can be dissolved in an appropriate solvent and examined either as a liquid in a cuvette or deposited onto a solid surface like silica gel, alumina,

or filter paper. Qualitative analysis of emission spectra is used to detect the presence of trace contaminants or to monitor the progress of reactions. Molecular applications include thin-layer chromatography (TLC) spot analysis, the detection of aromatic compounds, and studies of protein structure and membranes. Polymers are studied with regard to intramolecular energy transfer processes, conformation, configuration, stabilization, and radiation damage.

Many inorganic solids lend themselves to study by **PLY** to probe their intrinsic properties and to look at impurities and defects. Such materials include alkali halides, semiconductors, crystalline ceramics, and glasses. In opaque materials PL is particularly surface sensitive, being restricted by the optical penetration depth and carrier diffusion length to a region of 0.05 to several pm beneath the surface.

Emission spectra of impurity levels are used to monitor dopants in 111-V, 11-VI, and group IV compounds, **as** well **as** in dilute magnetic and other chalcogenide semiconductors. PL efficiency can be used to provide a measure of surfice damage due to sputtering, polishing, or ion bombardment, and it is strongly affected by structural imperfections arising during the growth of films like Sic and diamond. Coupled with models of crystalline band structure, PL is a powerful tool for monitoring the dimensions and other properties of semiconductor superlattices and quantum wells (man-made layered structures with angstrom-scale dimensions). The ability to work with low light levels makes it well suited to measurements on thin epitaxial layers.

Basic Principles

In **PLY** a material gains energy by absorbing light at some wavelength by promoting an electron from a low to a higher energy level. This may be described **as** making a transition from the ground state to an excited state of an atom or molecule, or from the valence band to the conduction band of a semiconductor crystal (electron-hole pair creation). The system then undergoes a nonradiative internal relaxation involveing interaction with crystalline or molecular vibrational and rotational modes, and the excited electron moves to a more stable excited level, such **as** the bottom of the
conduction band **or** the lowest vibrational molecular state.

If the cross-coupling is strong enough this may include a transition to a lower electronic level, such **as an** excited triplet state, a lower energy indirect conduction band, or a localized impurity level. A common occurrence in insulators and semiconductors is the formation of a bound state between an electron and a hole (called an exciton) or involving a defect or impurity (electron bound to acceptor, excitons bound to vacancy, etc.).

After a system-dependent characteristic lifetime in the excited state, which may last from picoseconds to many seconds, the electronic system will return to the ground state. In luminescent materials some or all of the energy released during this final transition is in the form of light, in which case the relaxation is said to be radiative. The wavelength of this emission is longer than that of the incident light. This emitted light is detected **as** photoluminescence, and the spectral dependence of its intensity is analyzed to provide information about the properties of the material. The time dependence of the emission can also be measured to provide information about energy level coupling and lifetimes. In molecular systems, we use different terminology to distinguish between certain PL processes that tend to be fast (submicrosecond), whose emission we **call** fluorescence, and other, slower ones ***(lo4*** s to **10** s) which are said to generate phosphorescence. The light involved in PL excitation and emission usually **Us** in the range **0.6-** 6 eV (roughly 200-2000 nm). Many electronic transitions of interest lie in this range, and efficient sources and detectors for these wavelengths are available. To probe higher energy transitions, UPS, ***XPS,*** and Auger techniques become useful. X-ray fluorescence is technically a high-energy form of PL involving X rays and core electrons instead of visible photons and valence electrons. Although lower energy intraband, vibrational, and molecular rotational processes may participate in PL, they are studied more effectively by Raman scattering and IR absorption.

Since the excited electronic distribution approaches thermal equilibrium with the lattice before recombining, only features within an energy range of -kT of the lowest excited level (the band edge in semiconductors) are seen in a typical PL ***emission*** spectrum. It is possible, however, to monitor the intensity of the PL **as** a hnction of the wavelength of the ***incident*** light. In this way the emission is used **as** a probe of the absorption, showing additional energy levels above the band gap.

DIELECTRIC ANALYSIS

The dielectric property is an important analysis in the field of research for the materials like crystals, alloys, glasses and electrically non-conducting samples. Each material has its own electrical characteristics which depend on the insulation or dielectric properties. The dielectric property is also related to the parameters like substrate impedance, loss and resonator frequency. Precise measurements of dielectric behavior for the materials can lead to reliable information to propose applications.

A material which has the capability to store charges or energy when applying an electric field is called dielectric. The complex dielectric constant contains two parts, which are real part and an imaginary part. They represent the capacity of storage and dielectric loss of the sample respectively. The dielectric constant or relative permittivity is defined as, the ratio of the capacitance with dielectric to the capacitance without dielectric. The value of dielectric constant (ε_r) is given by the formula,

$$\varepsilon_r = \frac{Ct}{A\varepsilon_0} \qquad (1.5)$$

where, A - cross-sectional area of the area, ε_0 - permittivity of free space, t - crystal thickness and C - capacitance.

The parallel plate capacitance method is used to analyze the capacitance and dielectric loss with respect to frequency. An alternating voltage is applied across the parallel plates which have a dielectric material in between. The schematic diagram of parallel plate capacitor is shown in Figure.

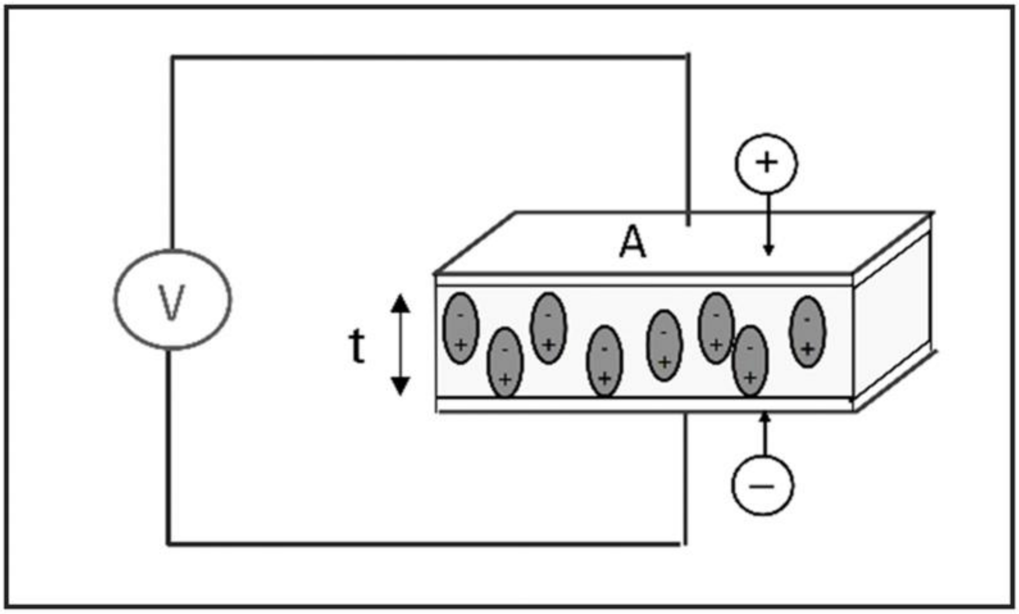

The schematic diagram of parallel plate capacitor

Dissipation factor or dielectric loss (D) is an energy loss in a dielectric sample due to applied alternating electric field. In other words, while the dipoles are rotating, a kind of internal friction arises to respond to the alternative electric field, which in turn gets converted as heat by the material. From the dielectric loss values, the quality, purity, deterioration or contamination of the material can be identified. The addition of external impurities or moisture can change the values of D. The conductivity of materials also depends on the value of dielectric loss factor.

There are four types of polarizations responsible for dielectric behavior, which are, space charge or interfacial, orientation, ionic and atomic or electronic polarization. The ionic and electronic polarizations are strongly independent of temperature and orientational and space charge polarizations are temperature dependent. Their response to external frequency depends on their inertia. At lower frequencies, having enough time to accumulate the charges, materials exhibit a higher dielectric constant values than at higher frequencies. The Figure 1.11 represents the variation of frequency versus polarization mechanism.

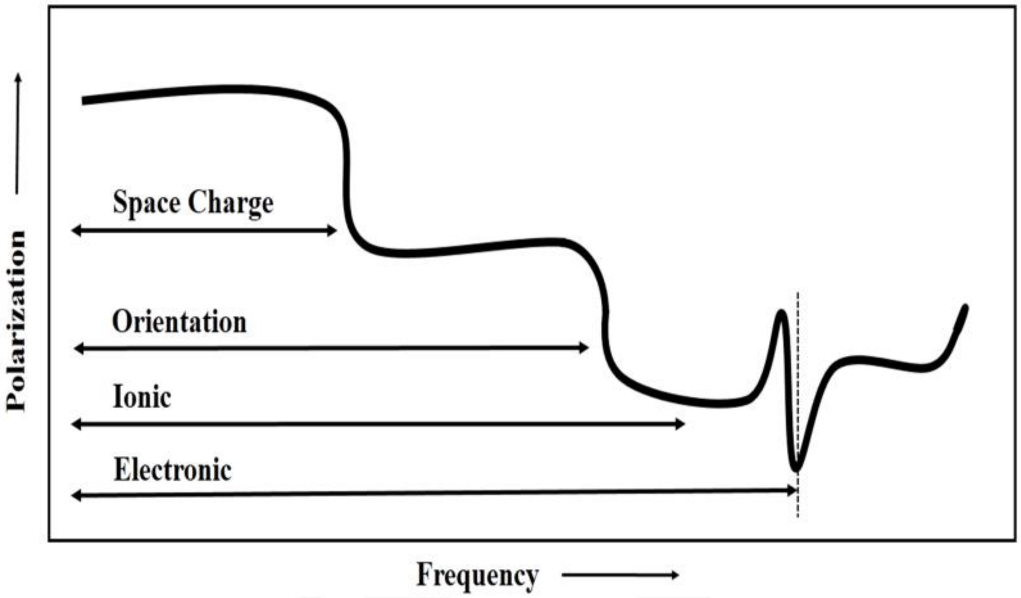

Variation of frequency vs polarization

KARPAGAM ACADEMY OF HIGHER EDUCATION, COIMBATORE-21
DEPARTMENT OF PHYSICS
CLASS : I M.SC PHYSICS
BATCH: 2018-2020
PART A : MULTIPLE CHOICE QUESTIONS (ONLINE EXAMINATIONS)
SUBJECT : MATERIAL CHARACTERIZATION
SUBJECT CODE : 18PHP105A
UNIT-V

SL.NO.	QUESTIONS	opt 1	opt2	opt3	opt4	Answer
1	Who coined the word 'nanotechnology'?	Eric Drexler	Richard Feynmann	Sumio Tijima	Richard Smalley	Eric Drexler
2	The size of nanoparticles is between _____ nm.	100 to 1000	0.1 to 10	1 to 100	0.01 to 1	1 to 100
3	"There is plenty of room at the bottom." This was stated by _____.	Eric Drexler	Richard Feynmann	Harold Croto	Richard Smalley	Richard Feynmann
4	Who prepared and explained nanotubes for the first time?	Sumio Tijima	Richard Smalley	Eric Drexler	Richard Feynmann	Richard Smalley
5	Carbon atoms make ____ type of bond with other carbon atoms.	covalent	ionic	metallic	hydrogen	covalent
6	Which of the following is an allotrope of carbon?	diamond	graphite	carbon nanotube	all of the above.	diamond
7	Fullerene or bucky ball is made up of ____ carbon atoms.	100	20	75	60	60
8	There are…… types of CNT	2	3	4	1	2
9	Which of the following statement/s is are true?	Volume to surface area ratio is very large for nanomaterials.	The cut-off limit of human eye is 10-5 m.	Hardness of a SWNT is about 63 x 109 Pa.	Carbon nanotubes are cylindrical fullerenes.	Carbon nanotubes are cylindrical fullerenes.
10	The thermal stability of a nanotube is seen up to ____ K in air.	100	1000	2000	3100	1000
11	The width of a carbon nanotube is ____ nm	1	1.3	2.5	10	1.3
12	In radial direction, the thermal conductivity of a nanotube is ____ watt/(m.K).	3500	385	350	0	0
13	The thermal stability of a nanotube is seen up to ____ K in vacuum.	100	1000	2200	3100	3100
14	The thermal conductivity of an SWNT along length is ____ watt/(m.K).	35	350	385	3500	3500
15	The tensile strength of an MWNT is ____ Pa.	63×10^6	63×10^7	63×10^8	63×10^9	63×10^9
16	The compressive strength of a nanotube _____ its tensile strength.	is less than	is greater than	is equal to	may be greater than	is less than
17	The hardness of a standard SWNT is ____ Pa.	63×10^6	25×10^6	25×10^9	25×10^{-9}	25×10^9
18	The bulk modulus of a standard SWNT is ____ that of diamond.	less than	greater than	equal to	less than or equal to	greater than
19	How much current can be passed through 1 cm^2 cross-section of a metal nanotube?	10^{-9} A	10^9 A	1000 A	0.001 A	10^9 A
20	The electrical conductivity of a nanotube is ____ times that of copper.	10	100	1000	1/100	1000
21	An MWNT possesses electrical superconductivity up to temperature of...	12 K	12°C	100 K	100°	12 K
22	The thermal conductivity of a standard SWNT along its length is ____ watt/(m.K)	3500	385	35000	35	3500
23	Nanoscience can be studied with the help of…	quantum mechanics	macro-dynamics	Newtonian mechanics	geophysics	quantum mechanics
24	Carbon nanotubes offer the advantage over metals of being:……	good electrical conductors	light and flexible	good absorbers of heat	strong.	good electrical conductors
25	Nanotubes usually form in bundles. Which is the best description of such a bundle?	The tubes are connected together by covalent C-C bonds	The tubes are randomly organized, with the axes of the tubes lying in random	The tubes are aligned, axes parallel, with van der Waals forces operating between	The bundles are of discrete sizes, and dipole-dipole forces hold the tubes	The tubes are connected together by covalent C-C bonds
26	The structure of SWCNT can be conceptualized by wrapping a………thick layer of graphite into a seamless cylinder	ten atom	two atom	one atom	none of the above	one atom
27	A single-walled nanotube (SWNT) can have a diameter of……… and a length of……	2nm,100µm	10nm,200µm	10mm,200µm	18nm,200mm	2nm,100µm
28	A single-walled nanotube (SWNT) can make a one dimensional structure called a………	nanodot	nanoclusters	nanoparticles	nanowire	nanowire
29	Carbon nanotubes can be made by……….	laser evaporation	carbon arc methods	chemical vapor deposition	all the above	all the above
30	In laser evaporation method, a quartz tube containing argon gas and a graphite target are heated to……..	100°C	1200°C	1000°C	500°C	1200°C
31	In laser evaporation, the……..sweeps the carbon atoms from the high-temperature zone to the colder copper collector	oxygen	CO_2	argon	hydrogen	argon
32	The…….. Method can produce single-walled nanotubes of diameters 1-5nm with a length of 1µm	carbon arc method	laser evaporation	CVD	PVD	carbon arc method
33	The ………method allows continuous fabrication and the most favorable method for scaleup and production	chemical vapor deposition	laser evaporation	carbon arc	PVD	chemical vapor deposition
34	Most MWCNTs have a diameter of close to………	100nm	10nm	1nm	1000nm	10nm
35	In …………..method a laser is aimed at a block of graphite	Laser ablation	Pulsed laser vaporization	CVD	both a and b	both a and b
36	In CVD, the synthesis of CNT is performed at …………. At atm. Pressure	1100°C	500°C	100°C	3000°C	1100°C
37	……………..method is used for the bulk production of SWCNTs	carbon arc method	laser evaporation	chemical vapor deposition	High-pressure CO conversion	High-pressure CO conversion
38	As the diameter of the nanotubes increases, the bandgap……………..	decreases	increases	remains same	a or b	decreases

39	Magnetoresistance is a phenomenon whereby the resistance of a material is changed by the application of a	AC magnetic field	DC magnetic field	DC electric field	none of the above	DC magnetic field
40	The decrease in resistance with increasing DC magnetic field is ……………	negative magnetoresistance	positive magnetoresistance	negative or positive magnetoresistance	none of the these	negative magnetoresistance
41	Carbon nanotubes have young's moduli ranging from ………….	2.8-3.8TPa	1.28-1.8TPa	1.28-1.8Pa	1.28-1.8MPa	1.28-1.8TPa
42	Young's modulus of carbon nanotubes is almost ………times that of steel	10	20	100	2	10
43	Carbon nanotubes have so…………….in their structure	many defects	few defects	moderate defects	all the above	few defects
44	The carbon-carbon bonds are……..	sp^2 hybrids	sp^3 hybrids	sp hybrids	sp^2 or sp hybrids	sp^2 hybrids
45	carbon nanotubes are about …….times stronger than steel	30	10	20	2	20
46	Single electron tunneling occurs when the capacitance of the nanotube is…….	so small	high	moderate to low	very high	so small
47	In the metallic state the conductivity of the nanotubes is ……….	very high	high	low	medium	very high
48	Carbon naotubes can carry a……….ampheres per square centimeter	trillion	million	billion	thousand	billion
49	nanotubes have a very high thermal conductivity, almost a factor of …… more than that of ………..	2, copper	4,diamond	2, silver	2, diamond	2, diamond
50	Advantages of carbon nanotubes on memory devices are	small diameter and low aspect ratio	low mechanical strength and aspect ratio	High aspect ratio and conductive along the axis	low conductivity and mechanical strength	High aspect ratio and conductive along the axis
51	Nano electronic devices using CNT can be manufactured using ………..	Bottom up approach	top down approach	both a and b	none of the above	Bottom up approach
52	Advantages of carbon nanotubes based biosensors……………	high specificity and sensitivity	fast response	slow response	both a and b	both a and b
53	………….is a powerful technique to calculate how tubes of different dia. Are distorted when placed on a substrate	molecular mechanics	biosensors	memory devices	none of the above	molecular mechanics
54	The diameter of nanotubes used to form the rings is ………..	3mm	1.4nm	5nm	100nm	1.4nm
55	The high ……………. Of CNTs means that they will be poor transmitters of electromagnetic energy	mechanical stability	thermal conductivity	electrical conductivity	none of these	electrical conductivity
56	CNTs are metallic or semiconducting, depending on the………………	diameter of the tube	chirality of the tube	temperature	both a and b	both a and b
57	There are a variety of structures of carbon nanotubes and these various structures have ……….properties	same	different	both a and b	none of the above	different
58	In carbon arc, carbon atoms are ejected from the…………electrode and form nanotubes on the……..electrode	positive, negative	negative,positive	either a or b	none of these	positive, negative
59	If no catalysts are used, the tubes are …………….	nested	multiwalled	single walled	either a or b	either a or b
60	The carbon arc method can produce ………………	MWNT	nested	SWNT	all the above	SWNT